# THE BEHAVIOR OF THE TRACE ELEMENTS IN COAL DURING PYROLYSIS

*Ruixia Guo, Jianli Yang, Dongyan Liu and Zhenyu Liu*

State Key Laboratory of Coal Conversion, Institute of Coal Chemistry
Chinese Academy of Sciences, P.O. Box 165, Taiyuan, Shanxi 030001, P.R. China

## Introduction

Coal is a cheap and the most commonly fuel in China. However, coal contains trace hazardous elements of environmental concerns in ppm order, such as As, Pb, Cr, Cd, and Mn. The presence of the elements can have a great influence on coal utilization processes. The most important effects are related to coal combustion and the environmental impact resulted from the thousands of tonnes of solid emitted into the atmosphere. For example, the release of the trace elements from coal as vapor or fine particles during combustion causes causes potentially toxic to plants, animals and human health and pollution to ecological environment under certain conditions and concentrations[1-3]. The formation of the technology for the coal utilization units requires the understanding of their occurrence in coal, their behavior during and prior to combustion and their form in the stack gas.

Recently, many of researchers have concentrated on behavior of trace elements during combustion and post-combustion[3-7]. Their investigation on the transformation of trace elements during coal combustion have shown that the volatility of trace elements depends on their affinities and concentrations, and on the physical changes and chemical reaction of these elements with sulfur or other volatile elements during combustion. The main purpose of this study is to understand the transformation of As, Pb, Cr, Cd, and Mn during coal pyrolysis. The effects of pyrolysis temperature and coal type were investigated. In addition, thermodynamic analysis was also further carried out.

## Experimental

Three Chinese coals, Datong, Shenhua and Yima, were used in this study. The coals were crushed and sieved to 0.16~0.27mm, and then dried under vacuum at 110°C with a nitrogen purge. The properties of coals are given in Table 1.

**Table 1. Analysis of coal samples•wt%**

| Coal sample | Proximate analysis | | | Ultimate analysis•daf | | | | | Ash analysis | |
|---|---|---|---|---|---|---|---|---|---|---|
| | $V_{ad}$ | $A_d$ | M | C | H | N | S | $O^a$ | Si | Al |
| Shenhua | 30.71 | 6.61 | 0.51 | 63.77 | 3.81 | 0.79 | 0.57 | 31.06 | 27.8 | 5.9 |
| Yima | 30.24 | 15.79 | 0.79 | 58.88 | 2.94 | 0.65 | 1.94 | 35.62 | 30.1 | 10.0 |
| Datong | 26.86 | 13.58 | 0.61 | 67.62 | 4.18 | 0.72 | 2.03 | 25.45 | 25.4 | 11.3 |

Note: a: by difference

Pyrolysis experiment was conducted in a fixed bed quartz reactor under $N_2$ stream with a heating rate of 20°C/min. The temperature ranges from 500°C to 1000°C. As, Pb, Cr, Cd, and Mn contained in char and raw coal were measured by inductively coupled plasma-atomic spectroscopy (ICP-AES). The concentrations of elements in three raw coals are presented in table 2. Bleeding ratio (BR) was defined as:

$$BR(\%)=\frac{\text{concentration in coal}-\text{concentration in char}\times\text{char yield}}{\text{concentration in coal}}\times 100\%$$

It was used to evaluate the change of the trace elements in coal during the treatment.

**Table 2. The concentration of trace elements in three coals•μg/g coal**

| Coal sample | As | Pb | Cr | Cd | Mn |
|---|---|---|---|---|---|
| Shenhua | - | 6.2 | 3.2 | - | 70.5 |
| Yima | 40.3 | 12.6 | 15.6 | 1.28 | 40.4 |
| Datong | 8.6 | 8.8 | 6.2 | 0.25 | 49 |

## Results and discussion

**Transformation of trace elements with temperature.** As shown in Fig 1(a), the large amount of As and Cd is released from Datong coal at relative low temperatures of 500°C, while the temperature for lead release is above 800°C. The lesser emission of Cr and Mn during pyrolysis implies that these elements may be retained by aluminosilicate, or was initially existed as more stable forms in raw coal[8].

The bleeding ratio was plotted versus the yield of volatiles (tar +gas) in Fig 1(b) for Datong coal. The points are divided into two parts by the diagonal line l. The points at the upper part represent the char with a concentration of trace elements lower than that in raw coal and the points at the lower part represent the char with a concentration of the trace elements higher than that in raw coal. As shows that the concentration of As, Cd and Pb in char decreased to lower than that in raw coal with increasing the yield of volatiles. This indicates that the majority of these elements vaporized by heat treatment. Cr and Mn concentration in all the chars, however, are higher than that in raw coal, which indicate their relative non-volatility.

**Effect of coal type.** The bleeding ratio of trace elements in 1000°C char with coal type is shown in Fig 2. This was examined for Pb, Cr, Mn in three coals and for As, Cd in Yima and Datong coals.

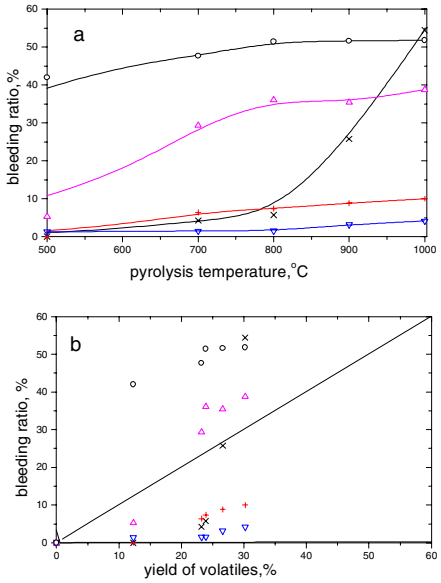


**Fig. 1** Effect of temperature on release of trace elements for Datong coal (o) As; (Δ) Cd; (×) Pb; (+) Cr; (∇) Mn

As indicated the bleeding ratios of Pb, Cr, Mn for Shenhua coal were the highest. Among the five trace elements considered, Lead was the most volatile element at pyrolysis temperature of 1000°C. Arsenic and cadmium were next volatile elements with bleeding ratio of 51.8% and 38.8% for Datong coal and 30.1% and 27.2% for Yima coal. For a given element, the bleeding ratio varies with the coal type. This may be caused by the difference in the chemical composition of the raw coal, both element-containing compounds and the relative compounds

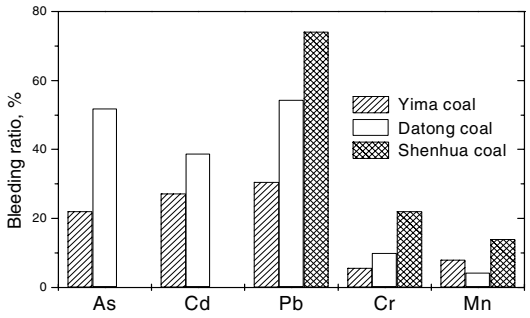


**Fig. 2** Effect of coal type on bleeding ratio of trace elements

**Thermodynamic behavior of trace elements.**

The element volatility behavior is related with boiling point of the element and of the relative compounds. The high volatility of the element is often related to the low boiling points and compounds. Boiling points of trace elements considered and their relative important compounds are presented in table 3. It can be seen that boiling points for Mn element and compounds are higher than the pyrolysis temperature studied. It is consistent with the lower bleeding ratio of Mn. Although the high boiling points of oxides, sulfides for Pb, Cr and Cd are relatively high, the boiling points of chlorides for these elements plus As are lower than the pyrolysis temperature range studied. Thus it may conclude that the formation of chlorides during pyrolysis promotes the emission of the elements. Due to high boiling points of element, oxide and sulfide, Pb is non-volatility. However, it can be transformed into Chloride at high temperature of 1100K by gasification-agglomeration effect[9]. This accelerates Pb emission. Moreover, this is consistent with the experimental result that bleeding ratio of Pb increased quickly above 800°C. As and Cd are both volatile elements based on the boiling points of elements and their oxides.

**Table.3. Boiling point of trace elementsand their compounds, °C**

| kind | Element | Oxide | Sulfide | Chloride |
|---|---|---|---|---|
| Pb | 1740 | 1535 | 1281 | 953 |
| As | 814 | 461 | 707 | 130 |
| Cd | 765 | >920 | 1382 | 964 |
| Cr | 2672 | 2275 | 1550 | 950 |
| Mn | 1900 | 1650 | | 1190 |

Furthermore, formation of their chlorides can also result in more emission for As and Cd from coal. However, the elements did not release completely during pyrolysis. This suggests that some of As and Cd may be existed in more stable structure in coal or chlorine content in coal is limited. Compared with Pb, As, and Cd, however, Cr is non-volatility element. This accords with the fact that high boiling points of element and compounds for Cr, especially that its chlorides is hardly to be formed at 1100K.

**Conclusions**

The behavior of trace elements observed in this study was dependent upon both coal type and pyrolysis parameters. The amount of trace elements emissed during pyrolysis increased with increasing temperature. Although Pb, As and Cd were volatile, their volatility varies with coal type. This indicates that the volatility is related with the form of the elements occurred in raw coal. Cr and Mn were relatively non-volatile elements under the conditions tested.

Further work identifying the relationship between volatile and elemental form in raw coal, particularly for the elements Pb, As, and Cd is clearly needed.

**Acknowledgement.** The authors gratefully acknowledge the financial support from the Special Founds for Major State Basic Research Project, the Chinese Academy of Sciences, and the Natural Science Foundation of China

.

**References**

(1) Eble, C. F.; and Hower, J. C. *Fuel*, **1997**, *76* (8), 711
(2) Feng, Xinbin.; Ni, Jianyu.; and Hong, Yetang. *Environmental Chemistry*, **1998**, *17* (2), 148.
(3) Swaine, D.J. *J. Coal Qual*. **1989**, *8*, 63
(4) Constance, L.S.; Lawrence, E.; Joseph, R.M. *Fuel Processing Technology*, **2000**, *63*, 109
(5) Querol, X.; Fernandez-Turiel, J.L.; and Lopez-Soler, A. *Fuel*, **1995**, *74* (3), 331
(6) Querol, X.; Juan, R.; Lopez-Soler, A.; and etc. *Fuel*, **1996,** *75*, 821
(7) Palmer, C.A.; Mroczkowski, S.J.; Finkelman, R.B.; Crowley, S.S.; and Bullock, J.H. In *Proceedings of the Fifteenth Pittsburgh Coal Conference (CD-ROM)*; 1998
(8) Raask, E. In *Mineral Impurities in Coal Combustion*; Hemisphere Publishing; London, 1985; pp.293-312.
(9) Wang, Xifen.; Sun, Xuexin.; and Li, Min. *Coal Conversion*, **1999**, *22*(1), 58

# CATALYTIC PYROLYSIS OF N-HEXANE FOR ETHYLENE PRODUCTION OVER MORDENITE ZEOLITES MODIFIED BY METAL OXIDES

*Jian Zheng[a], Jialu Dong[b], Weifeng Zhang[b], Qinhua Xu[b], Chunshan Song[a]*

[a] The Energy Institute & Department of Energy & Geo-Environmental Engineering, Pennsylvania State University, 209 Academic Projects Building, University Park, PA16802
[b] Department of Chemistry, Nanjing University, Nanjing 210093, P.R. China

## Introduction

Thermal cracking (pyrolysis, or so-called steam cracking) of various hydrocarbons at high temperature (1073-1123 K) for the production of lower $C_2$-$C_4$ olefins has been one of the core processes in the petrochemical industry. Besides the large amount of energy consumed in this pyrolysis process, another disadvantage is the difficulty for this process to control the olefins formed, especially the lower yield to ethylene. Therefore, pyrolysis of hydrocarbons in the presence of catalysts[1-6], allowing preparation of lower olefins at lower temperature and with higher selectivity, is a subject of some studies.

The search for catalysts that promote hydrocarbon cracking started in the late 1960s. Till now, the catalysts found active to different extent can be typically classified into three types, *i.e.*, acidic catalysts (amorphous silica-alumina or zeolite crystalline), basic catalysts (such as CaO-SrO-$Al_2O_3$, $KVO_3$/corundum etc.) and transition metal oxide catalysts (*e.g.*, $Cr_2O_3/Al_2O_3$), which are used under the non-aerobic or aerobic conditions[3]. Three catalytic pyrolysis processes, namely Vniios process in Russia (using $KVO_3$/corundum catalyst), Asahi process in Japan and the deep catalytic cracking (DCC) process in China (both using ZSM-5 zeolite modified with Al and Cr), have been developed[6]. However, they are still far from replacing the conventional pyrolysis technique, and it is therefore worthy exploring approaches to finding highly efficient catalyst system for preparing $C_2$-$C_4$ olefins.

In this work, we studied the acid-base and catalytic properties of a series of Mordenite zeolites for the pyrolysis of n-hexane, and modified the least acidic $Na^+$ type Mordenite by supporting basic metal (such as alkali, alkaline earth) and reductive transition metal oxides. The reaction mechanisms for different catalysts have been discussed.

## Experimental

**Sample Preparation.** Sodium-type Mordinite zeolite (NaM, the unit cell composition: $Na_{6.23}H_{0.02}Al_{6.25}Si_{41.75}O_{96}$) was purchased from HongGuang Molecular Sieve Co., Dalian, China. Three NaHM zeolite samples with different $H^+$ content were produced by ammonium ion exchange of NaM zeolite at 353 K for different times, each time for one hour, followed by calcinations at 773 K for 5 hours. Proper amount of alkali (Li, K, Cs), alkaline earth (Mg, Ca, Sr), and transition metals (Cu, Mo, Mn, Ag, etc.) oxides were introduced into NaM zeolite by impregantion of the respective metal nitrate solutions at 353 K, followed by calcinations at 973 K for several hours.

**Characterization.** The acidic and basic properties of Mordenite zeolites with or without metal modification were analyzed using $NH_3$-TPD and $CO_2$-TPD, respectively. Before the TPD experiments, all samples had been treated at 773K in $N_2$ for several hours. The adsorption of $NH_3$ or $CO_2$ was saturated at room temperature, followed by purging with $N_2$ at 333 K for at least one hour. TPD was then carried out at a heating rate of 12 K/min. The reduction of transition metal oxides was characterized by conventional TPR. All temperature-programmed studies were carried out using a TCD detector, and the TPD or TPR peak signals were recorded and calculated quantitatively.

**Catalysis**. Catalytic pyrolysis of n-hexane was performed in a continuous flow micro-reactor. N-hexane flew continuously through the catalyst together with steam, with the steam/hydrocarbon weight ratio to be 0.9 and the space velocity (WHSV) to be 3.6 $h^{-1}$. The reactor temperature was 808K for bare zeolite catalysts and 890K for metal oxide modified NaM catalysts. The reaction products after TOS of 1 h were analyzed by on-line gas chromatography with a TCD detector and Porapak Q column. Results were reported as conversions calculated as the weight percent of n-hexane reacted, molecular selectivity and yields, especially to ethylene.

## Results and Discussion

The curves of ammonia thermal desorption for NaM and three NaHM zeolites (figures not shown) exhibit mainly two peaks: low-temperature peak with $T_{max}$ at 497 K, typically representative of weak Lewis acid centers or cationic sites, and high-temperature peak with $T_{max}$ at 813 K, corresponding to strong Brönsted acid centers. It is found that, the higher temperature peak increases with the proton content in the NaHM zeolites, while the same peak can hardly be found in the case of NaM zeolite. **Figure 1** shows the catalytic pyrolysis results over the zeolites as a function of acidic amount, which was calculated from the amount of the $NH_3$-TPD peak at higher temperature. There is a clear trend that, with the increase of zeolite acidity, the activity increases while both the selectivity of ethylene and the ratio of $(C_1+C_2)/C_3$ decrease. This is due to the well-known cracking reaction on acidic catalysts, possibly via carbenium ion mechanism: the strong Brönsted acidic sites of NaHM zeolites protonate n-hexane to form carbenium ions, followed by β-scission to form smaller molecules. According to this mechanism, $C_3$ hydrocarbon and alkane would be the predominant cracking products rather than ethylene. Meanwhile, secondary undesirable reaction such as aromatization might occur between the olefin products and the carbenium ion intermediates, and coke formation becomes severe with the increase of strong acidity.

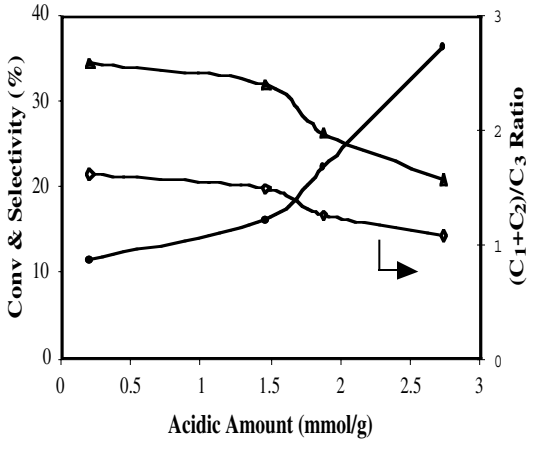


**Figure 1.** Catalytic pyrolysis (808 K) results of n-hexane over Mordenite zeolites with different acidic amount.
●: Conversion of n-hexane; ▲: Yield of ethylene
✧: $(C_1+C_2)/C_3$ Ratio.

In order to increase the ethylene selectivity, non-acidic NaM zeolite was selected, and basic metal oxide such as alkali (Li, K, Cs) and alkaline earth (Mg, Ca, Sr) were incorporated.

**Figure 2** shows results of catalytic pyrolysis over metal supported NaM zeolite catalyst as a function of base amount, which was calculated from the peak amount of the $CO_2$-TPD (pictures not shown). It is interesting to find that with the increasing basic sites introduced, both the activity and the yield to ethylene increase. This is because the catalytic cracking over non-acidic or basic catalysts with steam conditions follows a free radical mechanism, where the selectivity to alkene, especially ethylene, increases when compared with the carbenium ion mechanism on acidic catalysts.

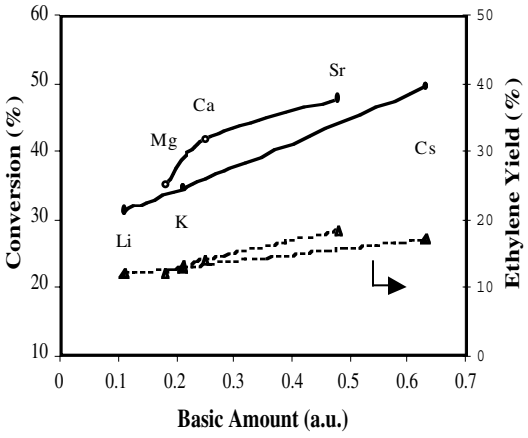


**Figure 2.** Catalytic pyrolysis (890 K) results of n-hexane over alkali and alkaline earth metal oxide supported Mordenite zeolites with different basic amount.
●: Conversion of n-hexane; ▲: Yield of ethylene.

TPR profiles of different transition metal oxide supported on NaM zeolites (pictures not shown) differ from one another because of the difference in both the electronic state and the reducibility of each metal oxide. For example, the reduction of CuO/NaM starts at about 500 K, while $MoO_3$/NaM can only be reduced at temperature higher than 870 K. It's therefore our intention to compare the catalytic cracking results of these catalysts as a function of their reducibility.

**Figure 3** shows the results of the catalytic pyrolysis over transition metal (Ag, Cu, Mn, Mo) oxides supported NaM zeolite as a function of the starting temperature of respective TPR peaks. It can be found that, the metal oxides that are easier to be reduced (except MnO) show approximately higher catalytic acitivity and yields to alkenes including ethylene. It has been reported that, catalytic cracking over non-reducible transition metal oxide catalysts such as $Cr_2O_3/Al_2O_3$ under aerobic conditions, *i.e.*, oxidative catalytic cracking, follows a free radical mechanism, where activated oxygen species abstract hydrogen from hydrocarbons to form radicals[3]. Accordingly, high yields of ethylene would be expected[3]. The present work does not involve $O_2$ during the catalytic pyrolysis. However, lattice oxygen in reducible transition metal oxide supported catalysts may exhibit the similar free-radical oxidative catalytic cracking of n-hexane. The easier the metal oxide to be reduced, the higher extent of this oxidative effect might have.

We also found that, if the transition metal oxide was reduced to metal, the catalytic activity decreased greatly. For example, the conversion of n-hexane over $PbO_2$/NaM and $VO_3$/NaM catalysts are 57.2% and 37.0%, respectively. But for Pb/NaM and V/NaM, they are only 10.8% and 3.6%, respectively. This shows again the importance for the existence of oxidative cracking.

**Table 1** shows the catalytic pyrolysis over the same transition metal oxide supported catalysts with or without steam. It can be seen that, in the presence of steam, the catalytic activity and ethylene selectivity decrease greatly. This indicates that steam plays an important role in keeping the transition metal oxides at higher oxidation state and therefore exhibiting the oxidative catalytic pyrolysis for n-hexane.

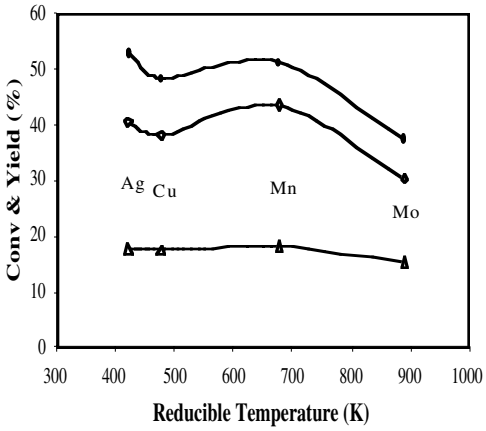


**Figure 3.** Catalytic pyrolysis (890 K) results of n-hexane over alkali and alkaline earth metal oxide supported Mordenite zeolites with different basic amount.
●: Conversion of n-hexane; ▲: Yield of ethylene.
✧: Total yields of alkenes.

**Table 1. Results of catalytic pyrolysis of n-hexane over $M_xO$ supported NaM in $N_2$ or $H_2O$ (890 K, WHSV 3.6 $h^{-1}$, $H_2O$/henxae ratio 0.9, TOS 1h)**

| Cat. | Conversion (%) | | $X_{C2H4}$ (%)* | | $Y_{alkene}$ (%)* | |
|---|---|---|---|---|---|---|
| | a | b | a | b | a | b |
| $Ag_2O$/NaM | 28.0 | 53.0 | 34.3 | 33.6 | 19.8 | 40.6 |
| CuO/NaM | 28.6 | 48.5 | 20.2 | 36.0 | 19.4 | 38.2 |
| MnO/NaM | 26.3 | 51.4 | 31.0 | 35.5 | 19.4 | 43.7 |
| MoO/NaM | 11.8 | 37.5 | 38.8 | 41.0 | 8.5 | 30.4 |

*$X_{C2H4}$: Selectivity to ethylene; $Y_{alkene}$: Yield of alkenes.
a: Reaction in $N_2$; b: Reaction in $H_2O$

**Acknowledgement.** We are grateful for the financial supports from National Natural Science Foundation of China, SINOPEC, and the Pennsylvania State University.

## References

(1) Le Van Mao, R.; Melancon, S.; Gauthier-Campbell, C.; Kletnieks, P. *Catal. Lett*. **2001**, *73*, 181-186.
(2) Erofeev, V. I.; Adyaeva, L. V.; Ryabov, Yu. V. *Russ. J. Appl. Chem.* **2001**, *74*, 235-237.
(3) Yoshimura, Y. et. al. *Catal. Surv. Japan*, **2000**, *4*, 157-167.
(4) Shi, Z.; Zhang, F.; Liu, S. *U.S. Patent* 6,211,104, April 3, **2001**.
(5) Xie, C.; Li, Z.; Shi, W.; Wang, X. *U.S. Patent* 6,210,562, April 3, **2001**.
(6) Picciotti, M. *Oil & Gas J.* **1997**, *97*, 53-58.

# A COMPARISON OF PRODUCT PROFILES FROM AQUEOUS PYROLYSIS OF SELECTED BIOMASS AND WASTE MATERIALS.

*Tanja Barth*

Department of Chemistry, University of Bergen, Allégaten 41, N-5007 Bergen, Norway

## Introduction

Conversion of biomass and waste into fluids could provide a sustainable alternative to increased use of fossil fuels. Alternatively, synthetic chemicals could be produced from renewable resources instead of petroleum, with a positive environmental effect. However, many types of widely researched processes of biomass pyrolysis do not give liquid products that are compatible with petroleum fluids. Since this would make the introduction of alternative fuels and raw materials much easier, a study of pyrolysis in an aqueous reaction medium aimed at optimising the yield of hydrocarbon-rich fluid products has been made.

Three types of clean vegetable biomass and five types of organic rich waste materials have been pyrolysed in batch reactors in the presence of excess water. Experimental designs covering a range of conditions with regard to temperature, duration, water content and catalysts have been used with the aim of maximising the yields of liquids, and providing a maximum of the hydrocarbon fractions or petroleum compatible liquids. The gas, organic-, aqueous and solid phase products have been fractionated, quantified and analysed to provide yield profiles and mass balances.

## Experimental

Batch pyrolysis experiments were performed in 21 ml stainless-steel autoclaves. The pyrolysis conditions were varied in the ranges given in Table 1. The biomass samples were clean wood and Miscanthus, various sewage sludges and industrial by-products. A fractional factorial design was used for each biomass type. 1 M aqueous solutions of KOH or NaOH were used as catalysts. Addition of zeolites and other solid catalysts were also tested. More than 200 experiments have been performed.

**Table 1: Pyrolysis Conditions**

| Parameter | Range |
|---|---|
| Temperature | 320 - 500 °C (mostly 340-380 °C) |
| Duration | 3 - 96 hours (mostly 6 and 17 hours) |
| Amount of biomass | 0.2 - 4 g (mostly 0.5 - 3 gram) |
| Amount of water | 0.5 -15 ml (mostly 2.2 - 9 ml) |
| Catalysts | |

The fluids were extracted and quantified gravimetrically, and fractionated into asphaltenes and oils by n-hexane precipitation and further separated in a silica micro-column to give hydrocarbons and a polar fraction. The coke yield was determined by weight and TOC measurements. The gas-phase and aqueous products were also analysed and quantified. A mass sum of recovered products was calculated from each experiment. Multivariate data analysis is used to relate the yield profiles to the experimental conditions.

## Results and Discussion

The product profiles are a function of the experimental conditions, with a high water-to biomass ratio giving a high yield of liquids relative to coke. The biomass stating material is, however, the dominating factor for the products. The maximum liquid yields are obtained from degraded sludges with high organic contents, while vegetable biomass produces more coke and asphaltenes, and relatively more of the polar fractions in the liquids. Figure 1 shows the liquid yields from 1 gram of four biomass types after pyrolysis at 380 ºC for 17 hours.

The reaction conditions can alternatively be optimised to give aqueous short-chain organic acids as the major product. Addition of a base together with excess water suppresses coke formation completely, but increases thee yields of aqueous organic acids and $CO_2$ by "capture" in the aqueous phase. Hydrocarbon gases are minor products at all conditions tested.

Addition of homogenous and heterogeneous catalysts changes the yield profiles significantly, but the effects are often not the same for the different starting materials. The addition of a base improves the yields from the vegetable biomasses, but has a slight negative effect for the sludges. The presence of potassium ion results in significantly improved hydrocarbon yields in most systems.

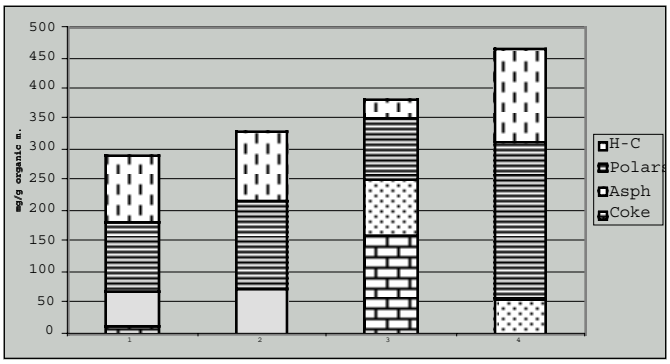


**Figure 1.** Examples of liquid yields from four biomass types at 380 ºC for 17 hours, with 1 g of dry biomass to 9 ml water in a 21 ml reactor.
H-C: Hydrocarbon fraction.
Sample 1: Clean woody biomass with 1 M KOH
Sample 2: Miscanthus stem with 1 M KOH
Sample 3: Sewage sludge from a chemical treatment plant with 1 M NaOH
Sample 4: Sludge from an industrial bio-filter with 1 M NaOH

## Conclusions

Solid biomass and organic wastes are converted to liquids in high yields by pyrolysis in autoclaves in excess water. The product is a petroleum-like fluid, but contains more non-hydrocarbon compounds than crude oils. However, the composition of the fluid is very dependent upon which raw material is being used, and on the reaction conditions. The following systematic relationships are observed from the experimental designs:

- The initial biomass composition determines the reaction pathways and product spectrum in pyrolysis in aqueous conditions.
- Degraded biomasses give the highest yields of fluids.
- Excess water as reaction medium increases the fluid yields for most biomass types.
- High carbohydrate biomass types produce high coke yields in the absence of potassium and base.
- Degraded biomass gives high fluid yields with no base added.

Further optimisation on specific raw materials has a good potential for providing petroleum compatible sustainable fuels.

**Acknowledgement.** Funding from the European energy research program JOULE (Contract JOR3-CT97-0176) is gratefully acknowledged.

# COPROCESSING OF YANZHOU COAL WITH A FCC SLURRY

*Z. J. Wang, J. L. Yang, Z. Y. Liu*

State Key Lab. of Coal Conversion, Institute of Coal Chemistry
Chinese Academy of Sciences, P.O. Box 165, Taiyuan, P.R.China

## Introduction

Although a number of processes for direct coal liquefaction and coprocessing of coal with petroleum resid have been developed to produce liquid fuels, the liquids produced are still expensive compared with petroleum[1]. Principal factors responsible for the high cost of coal derived liquids are the high cost of hydrogen, the severe liquefaction conditions and the use of expensive catalysts, which are essential for high yield of liquids[2]. Recently, a partial liquefaction concept was proposed [3], with characteristics of low-severity conditions and comprehensive utilization of all liquefaction products. In the partial liquefaction concept, high coal conversion to liquids is no longer necessary, highly active but expensive catalysts are no longer needed, however, use of the heavy liquefaction product becomes a key issue in the overall process. Following this thought, we recently studied the heavy liquefaction product and found that asphalt produced from coprocessing of coal and fluidized catalytic cracking (FCC) slurry under mild conditions meets the properties of high grade paving asphalt[4]. FCC slurry, produced from fluidized catalytic cracking process at oil refineries, has a relatively high polycyclic aromatics content. It is costly to further process it to produce distillates, but it is an effective solvent for coal liquefaction and is good for production of high grade paving asphalt[4,5].

This work investigates the coprocessing of coal with a FCC slurry under different reaction conditions. Coal conversions and product yields are studied to reveal the interaction between the coal and the slurry. The roles of catalyst and hydrogen are also discussed.

## Experimental

Yanzhou coal (Yanzhou, China) and a FCC slurry (Shijiazhuang oil refinery, China) were used. Their characteristics were shown in Tables 1 and 2.

**Table 1. Proximate and Ultimate Analyses of Yanzhou Coal**

| Proximate anal. W/% | | | Ultimate anal.W/% daf | | | | | |
|---|---|---|---|---|---|---|---|---|
| Mad | Ad | Vdaf | C | H | N | S | O* | H/C |
| 2.49 | 7.14 | 45.43 | 81.80 | 5.86 | 1.25 | 3.49 | 7.60 | 0.86 |

**Table 2. Ultimate Analyses of FCC Slurry**

| C | H | N | S | O* | H/C |
|---|---|---|---|---|---|
| 89.77 | 7.86 | 0.42 | 0.75 | 0.50 | 1.05 |

* by difference

Coprocessing experiments were performed under the following conditions: (1) $N_2$ atmosphere without catalyst, (2) $N_2$ atmosphere with a ferrous sulfate-based catalyst impregnated on coal[6], (3) $H_2$ atmosphere without catalyst, (4) $H_2$ atmosphere with a ferrous sulfate-based catalyst impregnated on coal. During a typical run, 100g mixture of coal and slurry were charged into a 1-liter autoclave. The reactor was filled with $N_2$ or $H_2$ to a pressure of 4 MPa and then heated up to 400 $^oC$ for reaction. After one hour reaction at 400 $^oC$, the autoclave was cooled with a fan to room temperature and the gases were vented. The liquid and solid products were collected and extracted with tetrahydrofuran(THF) and toluene(T) in sequence. The products were divided into following fractions: THF i(THF insolubles), preasphaltene(THF solubles, T insolubles), asphalt(>320 $^oC$ fraction of T solubles), oil(220-320 $^oC$ fraction of T solubles) and <220 $^oC$ fraction(including gases).

The THF and T conversions of coal were calculated based on coal(dry and ash free) and by subtracting contributions of the slurry. Product yields were obtained based on overall feedstock.

## Results and discussion

### THF and T conversions of coal

In order to understand the interaction between coal and slurry, Yanzhou coal was coprocessed with the FCC slurry at two different coal/slurry ratios(2:1 and 1:2) under the four reaction conditions mentioned above. The THF and T conversions of coal alone and product yields (based on the overall feed) under different conditions were determined to reveal the effects of slurry. The conversions of the coal are summarized in Table 3.

**Table 3. THF and T Conversion of Coal under Four Different Reaction Conditions**

| Conditions | THF conversion% | | | T conversion% | | |
|---|---|---|---|---|---|---|
| | coal * | (2:1) * | (1:2) * | coal | (2:1) | (1:2) |
| $N_2$, without cat | 16.9 | 17.3 | 32.0 | 15.8 | 16.5 | 1.5 |
| $N_2$, with cat | 15.5 | 16.5 | 21.1 | 14.4 | 15.3 | 8.2 |
| $H_2$, without cat | 38.3 | 62.8 | 71.8 | 35.3 | 44.8 | 27.4 |
| $H_2$, with cat | 57.5 | 70.8 | 85.2 | 44.2 | 48.2 | 42.7 |

* (coal) means the results determined coal alone , (2:1) and (1:2) denote the coal/slurry ratios in the feed.

It can be seen that the THF conversion increases with increasing slurry content in the feed concentration. The slurry enhanced dissolution and dispersion abilities to coal radicals and preventing them to combine together to form solid unreactive residue, which results in increased THF conversions. It is also observed that the increase in THF conversion is more obvious in $H_2$ atmosphere than in $N_2$ atmosphere, which may be caused by the good H-shuttling capacity of FCC slurry. However, it is somewhat surprising that the T conversion at coal/slurry of 1:2 is far lower than that at coal/slurry of 2:1. Possible reasons are that: At coal/slurry of 1:2 condition, the high content of slurry provides good dissolving and dispersing ability for coal and more coal radicals are stabilized as preasphaltene, which could not undergo further cracking and results in decrease of T conversion.

### Change of product yields in coprocessing under different reaction conditions.

In order to further understand the interaction of coal and slurry in coprocessing, theoretical product yields are calculated according to the product yields when coal and slurry are treated individually under the same reaction conditions. The differences between the experimental and the theoretical values, obtained by subtracting the theoretic value from the experimental value, are summarized in Tables 4 and 5.

**Table 4. Differences in product yields between experimental value and theoretical calculation in $N_2$ atmosphere**

| Condition | THF i | preasph- | asphalt | oil | <220$^oC$ |
|---|---|---|---|---|---|
| (2:1)* without cat | -0.2 | -0.1 | -10.2 | 2.6 | 8.0 |
| (2:1)* with cat | -0.6 | 0.1 | -13.0 | 1.6 | 11.9 |
| (1:2)* without cat | -4.8 | 9.5 | -8.4 | 0.5 | 3.2 |
| (1:2)* with cat | -1.7 | 3.7 | -9.1 | 1.3 | 5.8 |

* The meaning of (2:1) and (1:2) are the same as in Table 3.

In $N_2$ atmosphere (Table 4), less asphalt and more oil and <220 $^oC$ fraction are obtained in coprocessing, which means that there is a synergistic effect between the coal and the FCC slurry on production of oil and <220 $^oC$ fraction. It is also observed that, at coal/slurry ratio of 1:2, less THF insolubles and more preasphaltene were obtained, compared to those at coal/slurry ratio of 2:1, which suggests increased stabilization ability for coal radicals at high slurry content. However, more slurry also confines further cracking of coal radicals and leads to increased preasphaltene yield. It was found that addition of catalyst had no significant effect on changes of product yields in $N_2$ atmosphere.

**Table 5. Differences in product yields between experimental value and theoretical calculation in $H_2$ atmosphere**

| Condition | THF i | preasph- | asphalt | oil | <220$^oC$ |
|---|---|---|---|---|---|
| (2:1)* without cat | -15.8 | 9.2 | 4.4 | 1.7 | 0.5 |
| (2:1)* with cat | -7.7 | 5.6 | 4.5 | -1.8 | -0.6 |
| (1:2)* without cat | -10.0 | 13.2 | -0.5 | -2.0 | -0.7 |
| (1:2)* with cat | -7.9 | 9.0 | -5.8 | 0.4 | 4.3 |

* The meaning of (2:1) and (1:2) are the same as in Table 3.

Table 5 shows the differences in product yields in $H_2$ atmosphere. Results suggest that the coal and the FCC slurry have

a synergistic effect on decreasing THF insolubles. This is due not only to the increased dissolution and dispersion ability of slurry, but also to the good H-shuttling capacity of the slurry in the presence of $H_2$. It can also be observed that more preasphaltene was produced compared to that in the $N_2$ atmosphere. This again suggests that the enhanced H-donor ability hampered further cracking of preasphaltene. It is well known that the addition of catalyst can convert $H_2$ into active H atoms and promote the change of polyaromatics in the FCC slurry into hydroaromatics and the hydroaromatics promote cleavage of some strong bond in coal structure[7]. Therefore, in the presence of the catalyst, more hydroaromatics was produced from the slurry at coal/slurry ratio of 1:2 than at that of 2:1, which resulted in less asphalt and more oil and <220$^{o}$C fraction at coal/slurry ratio of 1:2.

**Conclusions**

1. Addition of the FCC slurry greatly enhanced coal conversion, which is attributed to its good H-shuttling capacity and dissolution ability for coal radicals.
2. Decrease of T conversion are observed when more FCC slurry is used in the coprocessing, the excessive FCC slurry may hamper further cracking of preasphaltene by stabilizing coal radicals.
3. In the presence of $N_2$, coal and FCC slurry have a synergistic effect on production of oil and <220 $^{o}$C fraction in coprocessing.
4. In the presence of $H_2$ and catalyst, polyaromatics of FCC slurry may be converted into hydroaromatics, which enhances H-donor ability and promotes the cleavage of strong bond of coal structure.

**Acknowledgement.** The authors gratefully acknowledge the financial support from the National Natural Science Foundation of China, the Chinese Academy of Sciences, and the Special Founds for Major State Basic Research Project. Mr. Yanti Wang of Shijiazhuang petroleum refinery is also acknowledged.

**References**

1 Osuma Okuma. Liquefaction process with bottom recycling for complete conversion of brown coal. Fuel, 2000,79,355-364
2 Derbyshire, F., Energy & Fuels, 1989,3,273-277
3 Liu Z. and Yang J. Proceedings of The Fifteenth Annual International Pittsburgh Coal Conference, September 14-18, 1998
4 Wang Z.J., Li Y. M., Zhang H. H. et al, Proceedings of the 10th International Conference of Coal Sciences [C]. 1999:1187-1190
5 Harrison G and Ross A B. Fuel, 1998,77,1421-1425
6 Zhang L.A., Yang J.L., Liu Z.Y., et al. Proceedings of the 10th International Conference of Coal Sciences [C]. 1999:965-968
7 Malhotra R, McMillen D F. Energy&Fuels, 1993,7:227-230

# DEVELOPMENT OF GASIFICATION/MELTING PROCESS FOR COAL AND COMBUSTIBLE WASTES

*Yongseung Yun and Ji Sun Ju*

Plant Engineering Center
Institute for Advanced Engineering
633-2, Goan-ri, Baegam-myeon
Yongin, Gyeonggi-do, 449-863 Korea

## Introduction

With recent widespread urgency in solving environmental problems, local environmental contamination in the past has become a serious worldwide problem in such forms as greenhouse effects, acid rain, and ozone depletion. In order to cope with these problems, many countries are trying to mandate to curb the amount of CO2 emission, to install facilities for reducing SOx, NOx in addition to regulate the use of CFC materials. Since the gasification can solve many of the current environmental problems even with energy recovery for wastes, many processes are unveiled during the last decade. In particular, recent interest in the gasification process itself that has been renewed in many developed countries yielded several noteworthy process developments for unconventional feedstock like biomass and municipal solid wastes.

Gasification research has been existed in Korea from late 1940's without much success. As in other developed countries, renewal of the technology starts just after the 1st oil crisis in the early 1970's even though they were basic studies. From 1990's, after the potential impact of IGCC (Integrated Gasification Combined Cycle) technology on the coal-utilizing power plants was recognized after the Cool Water project in USA, Korea started the small-scale process research. From 1993, pilot-scale gasification facilities were constructed in Korea and since then high-pressure gasification for the nine imported coals were performed. With the accumulated knowledge regarding the gasification, application area is being explored for waste feedstock from late 1990's in Korea.

Environmental concerns regarding the old-style coal-utilization and waste treatment technologies have prompted the development and application of gasification processes that produce far less pollutants like SOx, NOx and dioxins while recovering energy mainly as a chemical energy of CO and hydrogen. In Korea, coal needs to make up at least 1/3 of total generated electricity while waste incineration faces many challenges in convincing its environmental cleanness, especially with respect to dioxins and possibility of heavy metal leaching from the combustion ash. During the last eight years, Korea has prepared the application possibilities of gasification process into coal and wastes in that process cost and system availability were the main obstacles. In this paper, current research status of gasification research using coal and combustible wastes is discussed.

## Gasification Facilities

A dry-feeding entrained-bed type gasification facility, that is located at Ajou University in Suwon, Korea and can treat 3 ton/day at maximum 30 bar, 1650°C has been built in April 1995. **Figure 1** shows the facility (8 m x 17 m x 20 m) located in 30 m x 50 m space and the corresponding 3-dimensional PDS (Process Design System) picture. Main target feeds are subbituminous and bituminous coals, but petroleum coke is also possible to gasify. Coal feed is identical size with that of conventional power plants using pulverized coal, as 80-90% passing -200 mesh. Pulverized coal is pneumatically conveyed with nitrogen gas at dense-phase into the feeding nozzle system, where 99%-purity oxygen and steam are mixed with the coal powder. Steam is injected separately from the oxygen and coal powder.

Normal operation consists of the preheating, pressurization, transient operation, normal gasification operation, and the shutdown steps. LPG burner at the bottom of the gasifier did preheating of the gasifier at least for 20 hours. Then, nitrogen is introduced to pressurize the gasifier till the operating pressure range in less than 30 min, after this step, oxygen and coal powder are being fed into the gasifier. Coal supply is first started at the low feeding range in order not to cause any sudden pressure buildup in the gasifier and thus causing any back pressurization into the coal feeding lines. This step takes normally less than one hour. Normal hot test operation step for obtaining gasification data is maintained at the steady state for at least 4 hours to provide enough gas, slag, and other process data.

**Figure 2** show the view of the gasification facility that was being developed for the liquid or slurry type combustible wastes. Maximum pressure and temperature for the operation are 10 bar and 1550°C, respectively. Left-side view shows the waste-oil feeding facility including the heating lines for waste oils. Right-side view illustrates the main gasifier and the carbon scrubbing system.

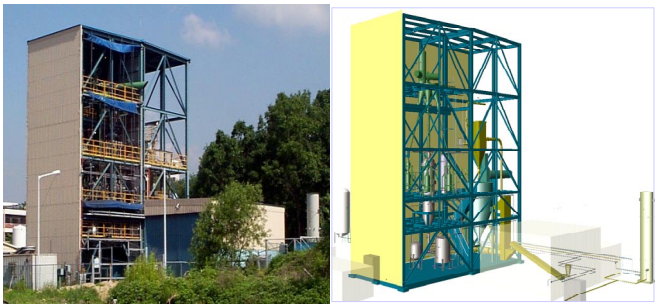

**Figure 1**. View of the 3 ton/day gasifier system and the corresponding 3-D design view.

**Figure 2**. Feeding facility (Left) and the gasifier section (Right) of the 1 ton/day-class waste-oil based gasification facility.

## Results and Discussion

Total 9 coals were tested under the high-pressure conditions of 12-29 bars and high temperature of 1400-1550°C. Important gasification parameters like carbon conversion and cold gas efficiency for the tested coals showed above 95% and 65-80%, respectively, depending on the coal used. [1]

Among coal properties influencing the gasification process, the removal rate of surface moisture content after drying was more important than the total moisture content in the coal feeding system. In the aspect of ash in coal, since most gasifiers remove ash as a molten slag, ash characteristics are one of the most important

parameters. Among the attributes of ash characteristics grasped in the study, a certain amount of ash in coal exhibits more favorable performance when judging from the experimental point of view.

From experiments that applied in coals of 2-11% ash content, due to satisfactory slag shapes and reasonable shape in coating refractory wall by tested coals, ash content of the coals proved to be in reasonable range for the application in the dry-feeding gasifier. Also, ash-melting temperature applicable in the dry-feeding gasifier was estimated to be better in the range of 100°C lower value than the gasifier reaction zone temperature of 1400-1500°C. That is, coals showing ash-melting temperature in the range of 1300-1400°C were thought to be best candidate coals for the slagging gasifier.

Most coals of bituminous and subbituminous rank, except coals of high fuel ratio (fixed carbon/volatile matter) and high ash content like Australian Curragh (VM 20.0%, FC 56.8%, Ash 16.1% as-received) and Russian Denisovsky (VM 20.1%, FC 59.1%, Ash 12.1% as received) coals, were all successfully applicable in the dry-feeding slagging-type gasifier.

Wastewater sludge was melted under combustion conditions yielding slags as shown in **Figure 3**. Left-side slag was obtained from the as-received feed ($CaO/SiO_2$=0.11) whereas the right-side slag that exhibits lower flow viscosity was produced after adjusting $CaO/SiO_2$ ratio as 1.0. Through the tests, self-reacting calorific value for the waste water in the facility was determined as 4,100 kcal/kg-ds, which is more or less higher than reported 3,500 kcal/kg-ds [2] probably due to the insulation depth of the reactor.

**Figure 3**. Slags obtained from wastewater sludge (unit: cm).

Inner structure of slag after gasification and ash after combustion was analyzed by XRD for the samples obtained from Australian Drayton coal as shown in **Figure 4**. While combusted ash samples show the crystal structure of $CaSO_4$, $SiO_2$, etc., slag samples exhibit an amorphous structure where all crystal structures in mineral matter were melted without much crystalline nature. Slags that were formed after melting under high temperature gasification temperature and solidification by cooling appear to bind the heavy metal components into the slag structure during the process. As demonstrated in **Figure 4**, heavy metal components appear to be intertwined with melted mineral matter components, so that the inner structure of slag is amorphous. According to the leaching tests on slags, Cu, Cr, Pb, Cd, As, Hg that are regulated as a heavy metal pollutants in a leached water in Korea were not detected at all. Thereby, coal slag can be safely utilized as a construction material or filler for road asphalt and proves not to cause any secondary pollution. Usually coal flyash from a boiler causes a secondary pollution by leaching.

One of the main focuses in the waste-oil based gasification is in minimizing soot production with minimum additional fuel to treat heavy metal containing wastes. More than 50% of waste-oil is reused through simple distillation as a fuel oil in Korea only for the designated boilers as a public bath place. Current obtained carbon conversion was 93% while the cold gas efficiency reached 71% for the waste oil. Another point is the control of residence time for different waste characteristics of melting temperature and slag viscosity for smooth slag discharge.

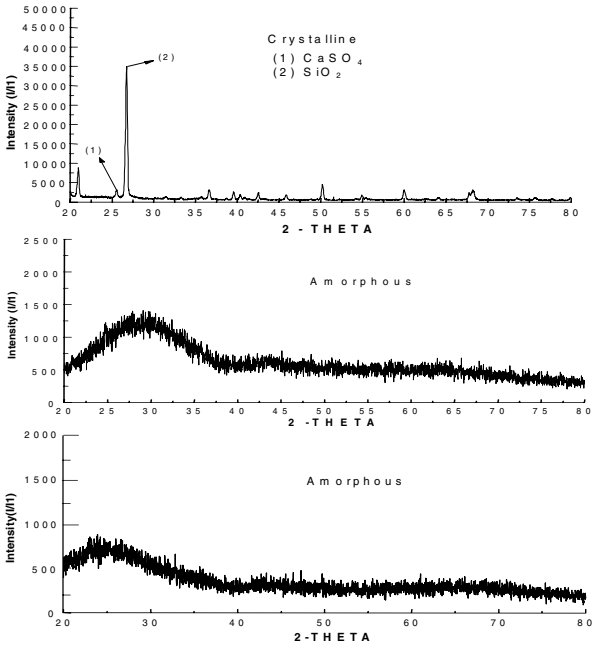


**Figure. 4**. XRD results of ash and slags from Drayton coal: combustion ash (Top) and slags (Middle: from 3 ton/day gasifier, Bottom: from commercial-scale gasifier).

## Conclusions

Slagging coal gasification pilot plant has provided the fundamental technologies that was a basis for the development of slagging combustor/gasifier using the waste feed like a sludge and waste oil. Coal gasification system yielded carbon conversion of above 98% and above 70% cold gas efficiency for the Indonesian subbituminous coals that were the best-suitable coals for gasification among the tested nine imported coals. Wastewater sludge was successfully treated at the developed combustion/melting process with above 90% slag-conversion and without any leaching problems of heavy metal components in slags. Gasification/melting process utilizing the calorific value of waste oil as a heating energy in melting has been installed and tested, in that powder-type wastes are converted into environmentally benign products with minimum extra fuel consumption. Developed combustion/melting process proved that designated-waste sludges can be treated cheaply compared to incineration, although general-waste-class sludges are yet to be competitive with conventional land-filling. Wide application of the technology requires more stringent environmental regulation that will in turn stimulate advanced process developments.

## Acknowledgement

This work was supported by KISTEP as one of National Research Lab. Projects in Korea under contract 2000-N-NL-01-C-224.

## References

1. Yun, Y.; Yoo, Y.D., *Korean J. of Chem. Eng.*, **2001**, 18(5), 679-685.
2.Greenhut, D.A.; Prepr. Pap.-*Society of Mining Engineers of AIME*, 1991, pp. 1-12.

# EFFECT OF GASEOUS ADDITIVES ON DESULFURIZATION OF COAL THROUGH PYROLYSIS

*Long Xu, Jianli Yang, Yunmei Li, Zhenyu Liu*

State Key Laboratory of Coal Conversion,
Institute of Coal Chemistry, Chinese Academy of Sciences,
Taiyaun 030001 P. R. China

## Introduction

With the increasing environmental concerns on $SO_2$ emission from coal combustion, use of high sulfur coals becomes more and more difficult. Development of sulfur removal process from coal prior to combustion is very important for continued used of high sulfur coals. Pyrolysis is likely to be an effective way to transform sulfur in coal to the gas and liquid phases, and to generate low sulfur content char for clean combustion.

Researches show that the efficiency of sulphur removal from coal through pyrolysis depends on many factors, such as temperature [1-3], heating rate [2], nature of atmosphere [3-6], residence time and coal type [6]. Pyrolysis of coals in nitrogen, hydrogen and steam indicates that $H_2$ atmosphere results in better sulphur removal efficiency than others, but the char yield is low, and the sulphur content of the char usually does not show significant decrease compared to the raw coal. To reach the goal of simultaneous sulphur removal and production of chars of high heating value, selective sulphur removal from coal is preferred. It is possible that addition of other chemicals are required to selectively reduce the strength of sulphur-carbon bonds and/or to stabilise the sulphur containing radicals to prevent them to form solid products, however, a little work is available in the literature in this field.

In this study, ethanol and acetone as well as nitrogen and hydrogen were used to constitute different atmospheres for pyrolysis of coal to evaluate their effect on sulphur removal. The results obtained are useful for understanding of sulphur removal mechanism from coal and for development of novel sulphur removal technologies.

## Experimental

A Spanish coal (Mequinenza) and three Chinese coals (Yanzhou, Datong and Xianfeng) were used in this study. All samples were ground to less than 0.25mm before use. Ultimate and sulfur-form analyses of the coals are presented in Table 1.

**Table 1. Ultimate and Sulfur-form analyses of sample coals**

| Samples | Yanzhou | Datong | Xianfeng | Mequinenza |
|---|---|---|---|---|
| Ultimate( wt%, daf) | | | | |
| C | 81.80 | 82.76 | 66.98 | 61.64 |
| H | 5.86 | 5.07 | 5.73 | 7.45 |
| N | 1.25 | 0.82 | 1.50 | 1.39 |
| S | 3.49 | 2.42 | 1.16 | 12.03 |
| O (diff.) | 7.60 | 8.93 | 25.63 | 17.49 |
| Sulfur-form (wt% total ) | | | | |
| Pyritic | 44.70 | 64.32 | 2.59 | 3.82 |
| Sulfate | 0.57 | 3.01 | 14.66 | 9.39 |
| Organic | 54.73 | 32.67 | 82.76 | 86.79 |

Pyrolysis runs were carried out in a fixed bed quartz tube reactor (70cm length, 1.4cm i.d.). Coal samples were heated from room temperature to 500°C or 700°C at a heating rate of 10°C/s. Ethanol or acetone was fed into the reactor by a pulseless pump, vaporised and then carried to the pyrolysis area by nitrogen. As a reference, hydrogen atmosphere was also used in the study. And the flow rate of nitrogen or hydrogen was 30ml/min. In order to compare the effects of different atmospheres, the same amount of organic reagents as that of hydrogen (in mol) were introduced. The amounts of these reagents actually fed into the reactor were 0.05ml/min for methanol, 0.08ml/min for ethanol and 0.10ml/min for acetone in the liquid state.

The sulfur content of raw coals and the pyrolysis chars were analysed by a sulfur detector (model WDL-3C).

## Results and Discussion

Figures 1(a, b, c, d) is the desulfurization results of these four coals at 700°C. In the figure, X-axis represents the percentage changes of the weight loss of coal (weight lose%), and Y-axis is the corresponding efficiency of desulfurization (De-S%). By this way, the degree of desulfurization can be reasonable evaluated. For a pyrolysis in which De-S% is equal to the weight loss%, in other words, the sulfur content in char ($S_{char}$%) is as same as that in coal, then the result is represented by a point on the diagonal line.

Figure 1(a) is the effect of atmospheres on desulfurization of Yanzhou coal. It shows that for Yanzhou coal the order of the effect on De-S% is as following $H_2$>$N_2$> $C_2H_5OH$> $CH_3COCH_3$. However, the value of weight loss% is also with the similar order. Furthermore, the values of $S_{char}$% are 2.56% for $H_2$, 2.77% for $N_2$, 2.54% for ethanol, 2.79% for methanol, and 2.87% for acetone. Although the values of $S_{char}$% for hydrogen and ethanol atmospheres are very similar, the yield of char for ethanol is about 7 percentage points higher than that for $H_2$ atmosphere. This suggests that ethanol atmosphere is much more selective to sulfur removal than $H_2$ atmosphere. It is also interesting to note that introduction of acetone also results in higher char yields compared to that in $H_2$ and $N_2$ atmospheres. Figure 1(b) is the desulfurization results of Datong coal. Among the four atmospheres, ethanol results in the highest char yield and the highest De-S%. While De-S% and the char yield observed for $H_2$ atmosphere are nearly 20 and 7percentage points lower than that for ethanol, respectively. Figure 1(c) is the pyrolysis results of Xianfeng coal. Again, ethanol atmosphere results in almost the highest De-S% and nearly the lowest weight loss%. Figure 1(d) is the results of Mequinenza coal. Similar to the Chinese coals, ethanol atmosphere gives the highest char yield and the highest De-S%. Although $H_2$ atmosphere yields a De-S% value very close to that of ethanol atmosphere, its weight loss% and $S_{char}$% are higher than that in ethanol atmosphere.

In general, Figures 1 shows that introduction of ethanol and acetone does alter the pyrolysis of the coals, and usually results in the chars with high yields and low sulfur contents. Hydropyrolysis, on the other hand, usually promotes devolatillazation of coal but is ineffective to generate low sulfur-containing chars.

Although detailed mechanism on the effect of the atmospheres is not clear by now, it is certain that this effect is related to the state of sulfur in coal as well as the type of the coal. The differences in weight loss% between ethanol and hydrogen for Yanzhou, Datong, Xianfeng and Mequinenza are 7.21%, 6.94%, 3.17% and 3.18%, respectively. The four coals studied can be divided into two groups, one group are lignites, including Mequinenza and Xianfeng, the other are bituminous coals, while the differences mentioned can also be divided into two groups, 3% for lignites and 7% for bituminous coals. The phenomena may indicate that the influence of ethanol on yield of char is related to the type of coal or carbon content in raw coal. Comparing the desulfurization efficiency of these coals, it was observed that the improvement of De-S% by ethanol atmosphere is much more than those by hydrogen atmosphere for Datong coal. It suggests the possible existence of the special sulfur containing structures in Datong coal, which interact strongly with ethanol during pyrolysis.

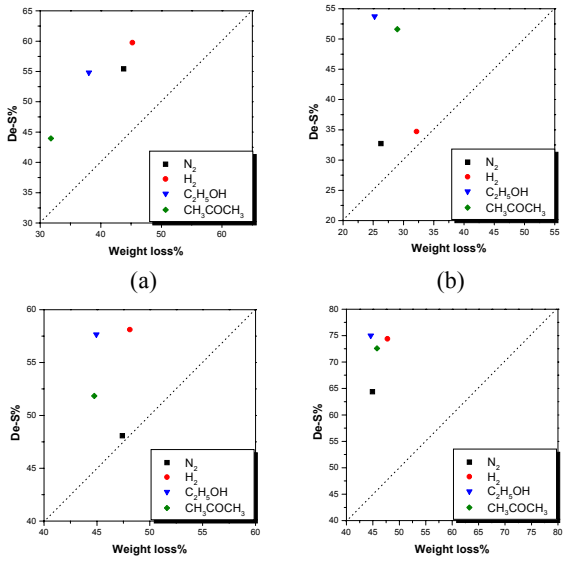


**Figure 1.** Effect of gaseous additives on desulfurization of four coals during pyrolysis. (a) Yanzhou coal (b) Datong coal (c) Xianfeng coal (d) Mequinenza coal

In order to see clearly the effects of the gaseous additives at different temperature ranges during pyrolysis, a variables $F_T$ is used in this study. $F_T$ and is calculated according to the following equation:

$$F_T(T1\sim T2)=[(De\text{-}S\%_{T2}-De\text{-}S\%_{T1})/(Weight\ loss\%_{T2}-Weight\ loss\%_{T1})]\text{-}1$$

Based on the equation, if the change of De-S% is dominant, then $F_T$ will be more than zero, but if the change of Weight loss% is dominant, then it will be less than zero. Here two temperature ranges, ≤500°C and 500~700°C, are studied separately. Figure 2 is the change of $F_T$ for Yanzhou coal in different pyrolysis atmospheres. It is observed that: (1) Below 500°C, the value of $F_T$ is more than zero only for ethanol, zero for acetone and less than zero for the others. That is to say, in the atmosphere of ethanol more sulfur can release than volatile matter does. While in other atmospheres the emission of volatile matter is dominant; (2) From 500°C to 700°C, all $F_T$ is more than zero. That is to say, sulfur releasing is dominant in this temperature range for all atmospheres. And in hydrogen the desulfurization effect is the best. In acetone and ethanol there are similar effect on desulfurization; (3) In hydrogen the gap of $F_T$ between these two temperature ranges is the widest, while in ethanol the gap is the narrowest. The atmosphere of hydrogen is the most sensitive to temperature, while ethanol is a relative mild atmosphere for desulfurization. Of course, $F_T$ is only the overall effect in the temperature range, and if the temperature range is narrow enough, the nature of each atmosphere will be discovered more clearly.

**Figure 2.** The change of $F_T$ for Yanzhou coal under different pyrolysis atmospheres.

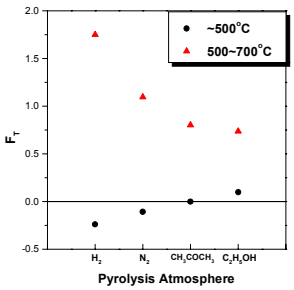


The promotion on sulfur removal by the introduction of ethanol depends not only on the sulfur structure in coal, but also on the decomposition of itself during pyrolysis. As known, pyrolysis generates free radicals from coal under a broad range of temperatures. Combination of large radicals produces heavy products such as char, and combination of small radicals produces volatile products such as gas and tar. If there is not enough small radicals to stabilizing the sulfur-containing radicals from coal, the sulfur-containing radicals released from coal may react with large radicals to form char, which reduces the sulfur removal effect. Pyrolysis of the organic reagents added may produce more small radicals including hydrogen redicals, to stabilize the sulfur containing radicals, and to increase the amount of sulfur in the volatile products. The proposed decomposition mechanisms of ethanol and acetone are shown in the following along with the decomposition energy for each substance.

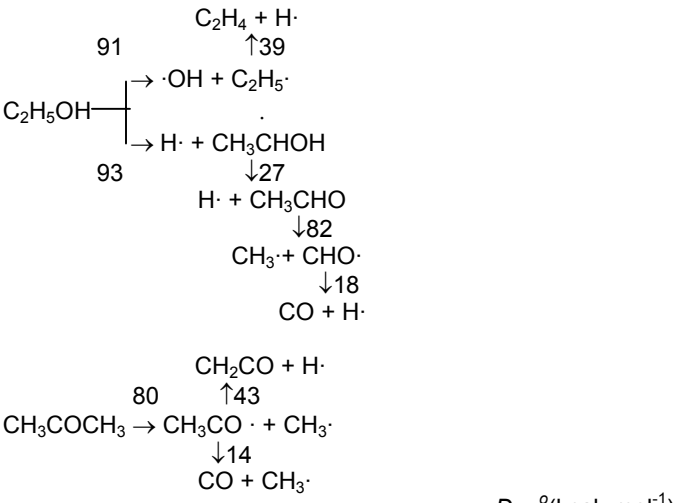


Comparing these reactions, it is observed that ethanol can generate more small free redicals, especially hydrogen redicals, than acetone. Among these free radicals, hydrogen redicals may be the main one promoting the sulfur removal reaction. Studies, however, are needed for further exploration on this subject.

## Conclusions

Compared to pyrolysis and hydropyrolysis of coals, the introduction of ethanol and acetone into the reaction atmosphere selectively promotes sulfur removal from coal, which results in chars of low sulfur content and high yield, especially for ethanol. In addition, there is a symmetrical and promotive effect on desulfurization at a wide temperature range in ethanol.

**Acknowledgement.** The project is subsidised by the Special Founds for Major State Basic Research Project, the Chinese Academy of Sciences, and the Natural Science Foundation of China and Shanxi Province, and the State Key Laboratory of Coal Conversion.

## References

(1) Kelemen, S. R.; Gorbaty, M. L.; Geoge, G. N.; Kwiatek, P. J.; Sansone, M. *Fuel*, 1991, ***70***, 396-402.
(2) Sugawara, K.; Tozuka, Y.; Sugawara, T.; Nishiyama, Y. *Fuel Processing Technology*, 1994, ***37***, 73-85.
(3) Liao, H. Q.; Li, B. Q.; and Zhang, B. J. *Fuel*, 1998, *77*, 1643-1646.
(4) Chen, H. K.; Li, B. Q.; Yang, J. L.; Zhang, B. J. *Fuel*, 1998, *77*, 487-493.

(5) Robert, S.; and VanMeurs, P. *Fuel*, 1980, ***59***,458-464.
(6) van Heek, K. H.; and Hodek, W. *Fuel*, 1994, ***73***, 886-896.

# ELECTROCHEMICAL PROPERTIES OF MCMBS AS ANODE FOR LITHIUM ION BATTERY

*Baohua Li, Ruixia Guo, Kaixi Li, Chunxiang Lu, Licheng Ling*

State Key Laboratory of Coal Conversion, Institute of Coal Chemistry, Chinese Academy of Sciences, P.O. Box 165, Taiyuan, Shanxi 030001, P.R. China

## Introduction

It is recognized that lithium secondary batteries using lithium metal exhibit problems, which make it difficult for their wide usage in consumer market. The problem is the unsafe characteristic, such as combustion and explosion due to dendrites formed at the surface of lithium metal during charge-discharge cycles. To solve this problem, a "rocking-chair" battery, which uses another intercalation compound as the anode for the lithium secondary battery, has been proposed. Among the alternative materials, which could replace lithium metal as the anode, the carbon materials are very desirable from the viewpoints of being abundant. Carbon materials have received much attention as anode material for lithium ion batteries since 1990. Various carbon materials have been investigated and shown good performances as the host for lithium [1-7]. They have high reversible capacity, high cyclic efficiency(ca,100%) , low electrochemical potential (•1V vs .Li/$Li^+$ ) and long cycling life.

The theoretical lithium storage capacity of a graphite anode for a lithium secondary battery has been considered to be 372mAh/g, corresponding to the first stage Li-GIC (Lithium-graphite intercalation compound, $LiC_6$). To further increase the energy density of lithium secondary batteries requires increasing the specific capacities of the electrode materials. Mesophase microbead (MCMB) prepared from petroleum pitch or coal tar is one of the candidate carbon materials available commercially. since it has high specific capacity(•500 mAh/g) and a spherical structure[4] which can be easy for closely packing, resulting in high density of electrode. Its low surface area can also minimize the side reactions during charge-discharge process. The present work studied the charge-discharge properties of MCMBs with different mean diameter and size distribution.

## 2 Methods

**2.1 Preparation of MCMB.** MCMB was prepared by heat-treating coal tar pitch with 3.7%wt pyridine insoluble fraction (PI) at 723K for 1~4h under autogenous pressure. Mesophase pitch was filtrated at 423K. The residue was then extracted by pyridine to get MCMB, which was further carbonized at 973K for 1h under $N_2$.

**2.2 Analyses of SEM.** The surface morphology of the isolated spherule after heat-treatment at 973K was observed under scanning electron microscope (Hitach H-600).

**2.3 Electrochemical measurement.** Working electrodes were fabricated by mixing MCMB with 10% wt of binder poly-[tetrafluroethylene](PTFE) and were dried at 433K under vacuum for 12 h in a dry box.

Electrochemical measurements were performed by using three-electrode cells. Carbon electrode was used as work electrode. Lithium metal was used as a counter electrode and a reference electrode. The electrolyte was 1MLiPF6-EC/DEC (volume1: 1) solution. All the operations on the cells assembled were carried out in the glove box filled with argon gas. Galvanostatic cycle was carried out at a constant current density of 15mA/g, and the cut off range is from 0.001 to 2V vs $Li/Li^+$.

## 3 Results and discussion

**3.1Features of isolated spherules (MCMB).** SEM photographs of MCMBs prepared under different conditions are shown in Fig1 (a)-(d), and the diameter distributions of MCMBs are shown in Fig 2. Fig1 shows that the diameter of MCMBs increased significantly with increasing reaction time. Fig2 shows that the diameter distribution of samples a, b and d are almost normal frequency distribution, while sample c has a few small MCMBs and large number of relatively big MCMBs.

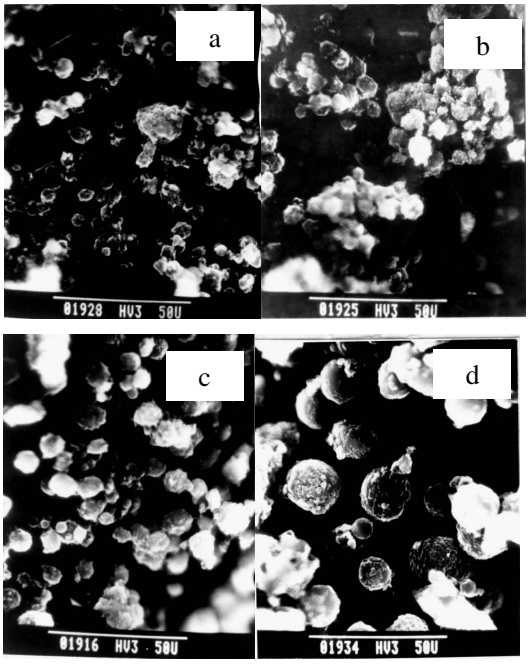


**Fig. 1** SEM photographs of MCMBs prepared under At 723K for different time, a 1h, b 2h, c 3h, d 4h.

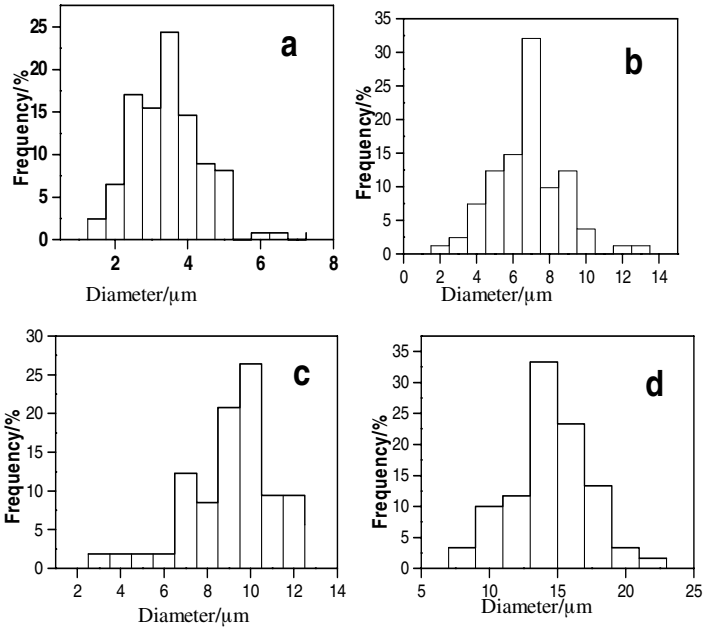


**Fig 2**. The diameter distribution of the MCMBs derived from coal tar pitch at 723K for different time, a 1h, b 2h, c 3h, d 4h.

**3.2 Electrochemical properties of MCMBs .** Fig 3 showed the first cycle charge-discharge profiles of MCMBs. The plateau observed at 0.8V vs $Li/Li^+$ during charge was attributed to the formation of solid electrolyte interface film (SEI) by the decomposition of electrolyte. Fig3 showed that the discharge profiles of MCMBs had a large hysteresis and a potential plateaus appearing at approximately 1V vs $Li/Li^+$, while the charge profiles had no potential plateaus appearing at approximately 1V vs $Li/Li^+$. Accordingly, the plateau is not due to a side reaction such as electrolyte decomposition but the cavities, which came into being when MCMBs were heat-treated at 973K. Lithium ions stored in the cavities were de-inserted at about 1V $Li/Li^+$[4].

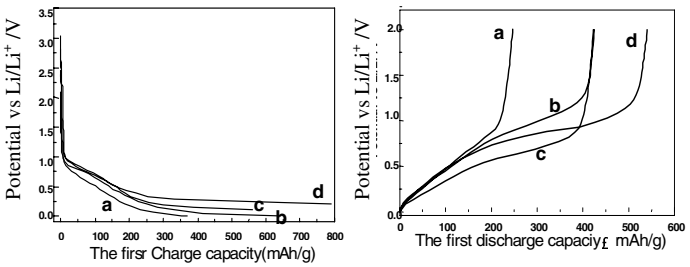


**Fig 3**. The first charge-discharge curves of MCMB heat-treated at 973K

Table 1 summarized some properties of MCMB anode., The first reversible capacity increased from 246 to 541 mAh/g with increasing of the mean diameter. And the first coulombic efficiencies were respectively 66.4%, 66.0%, 75.7%, and 68.3%. Since small MCMB has large specific surface area, resulting in more SEI, the first coulombic efficiencies increased with increasing of the mean diameter of MCMB. However, for the large MCMB, the numbers of rupture and defects will increase. When lithium ion diffuses into the large particle, it is probable to come across more ruptures and defects, making the diffusion dynamics process difficult. This gave rise to more irreversible capacity. Moreover, the interface of MCMBs decreases with increasing of particle size, which may reduce the electrical conductivity of MCMB. Consequently MCMB's cyclical property draws down. For example, the second discharge capacities of sample a, b, c and d, are respectively 8, 14, 22, 80 mAh/g less than the first cycle. If proper proportion of small MCMBs is added to big MCMBs, the electrical conductivity will be improved. This can be noted in Figure 3 and Table 1.The size distribution of sample c makes charge-discharge property fine. The first/second discharge capacity was 424/402 mAh/g and the first coulombic efficiency was 71.7%.

**Table 1. Some properties of MCMBs prepared from coal tar at 723K**

| Code | Heattreatment time (h) | Mean diameter ( μm) | First /second Cr(mAh/g) | First Cirr (mAh/g) | First coulomic efficiency(%) |
|---|---|---|---|---|---|
| a | 1 | 3.2 | 246/238 | 124 | 66.4 |
| b | 2 | 6.5 | 425/411 | 219 | 66.0 |
| c | 3 | 8.9 | 424/402 | 167 | 71.7 |
| d | 4 | 13.8 | 541/461 | 243 | 68.3 |

Cr- reversible capacity Cirr-irreversible capacity

## 4 Conclusions

MCMB is one of the promising carbon materials as anode for lithium secondary battery among commercially available carbon materials. The MCMBs heat-treated at 973K had higher reversible capacity than the theoretical lithium storage capacity of a graphite anode. This suggests that there be a cavity mechanism for the charge-discharge reaction. The mean diameter and size distribution of MCMBs have influence on the charge-discharge properties of MCMBs.

**Acknowledgements**.The project is supported by Shanxi Province Natural Science Foundation • 991068 • and Chinese Academy of Sciences Foundation and State Key Laboratory of Heavy Oil Processing in the University of Petroleum • 199901 •

## Reference

(1). Pled, E.; Menzchem,C.; BarTow, D. and Melman, A.. *J. Electrochem .Soc*, **1996**, *143*(1), L4-L7
(2). Ishikawa,M.; Kamobara,H.; Morita M. et al, *Journal of Power Sources*, **1996**, *62*, 229-232
(3). Buiel, E.; and Dahn, J.R. *J. Electrochem.Soc,* **1998**,*145*(6), 1977-1981
(4). Mabuchi,A.; Tokumisu, K.; Fujimoto, H.; and Kasuh, T. *J. Electrochem. Soc,* **1995**,*142*(4), 1041-1046
(5). Naji, A.; Willmann, P.; and Billaud, D. *Carbon*, **1995**,*33*(9), 1347-1352
(6). Liu,Y.; Xue, J.S.; Zheng, T.; and Dahn, J.R. *Carbon* , **1996**,*34*(2),193-200
(7). Bondarenko, G.N.; Nalimova,V.A.; Fateev, O.V. *Carbon*, **1998**,*36*(7-8), 1107-1112

# Hydrotreatment of tar formed in gasification of biomass

*M. Hernelind[+] and B. Gevert[*]*

*Department of Applied Surface Chemistry, Chalmers University of Technology, S-412 96 Göteborg, Sweden.*
[+]Present address: Perstorp AB, S-284 80 Perstorp, Sweden.
[*]Corresponding author. Tel.: +4631-7722956; fax: +4631-160062; e-mail: gevert@surfchem.chalmers.se

## Introduction

Gasification of biomass leads to more or less production of a tar. A lot of research has bean done to crack this tar into carbon monoxide and hydrogen. In this paper we will present an alternative way of using the tar. The purpose with here is to present some results of stabilizing tar from gasification of biomass by hydrotreatment with a commercial CoMoS-catalyst. We are here focusing on finding the optimum temperature for hydrodeoxygenation (HDO) of the tar. The effects of pressure and liquid hourly space velocity (LHSV) are also studied. The results are based on five analysis methods: elemental analysis, $^{1}$H-NMR, FT-IR, GC and water content analysis.

## Experimental

The raw material for this study was tar formed in a gasification plant in Tervola, Finland. The type of gasifier was a mixture of up- and down-draught. To pump the tar through the continuous hydrotreating system a piston pump was used. The tar was filtered with three sieves with the mesh sizes of 710 µm, 125 µm and 45 µm. In this study a commercial CoMo catalyst called Akzo Ketjenfine 702 was used. The catalyst was sulfided in the reactor by exposing the catalyst to a gas mixture of $H_2/H_2S$ 90/10% by volume. The hydroprocessing system study consisted of a feed tank, a reactor and a separator, which were connected to each other by _-inch stainless steel pipes (REF REACYTOR). Since Baker et al. (1) used up-flow mode for upgrading flash pyrolysis tar in their hydroprocessing apparatus to prevent reactor bed blocking, that mode was also used here. The reactor was filled with 40 ml of catalyst.

## Results and Discussion

**Analysis of the gasification tar.** The properties of the feed tar formed in gasification of biomass are reported in Table 1. The water content was 8.14 %, which is relatively low compared to bio-oils produced by fast pyrolysis. The water in the tar together with the water produced by the hydrodeoxygenation reactions deactivates the hydrotreating catalyst in two ways. Water molecules may, according to Furimsky (3), adsorb to anion vacancies and thereby block active sites and Grange et al. (4) reports that water also alters the structure of $\gamma$-$Al_2O_3$ support materials. If the $\gamma$-$Al_2O_3$ is hydrated into the boehmite phase the characteristic porous structure will be lost. The reactants will then have reduced access to active elements in the support material. However, water in bio-oils also lowers the viscosity and makes the bio-oils more stable. Moreover the elemental analyses showed that the tar contained less oxygen than bio-oils from fast pyrolysis, which have a typical oxygen content of 44-46% by weight including the oxygen in the water. The GC analysis showed that the amount of compounds in the lighter fractions of the tar was relatively small. In the IR spectrum of the tar, which is reported in Fig. 2, it can be seen that the tar was a cocktail of different hydrocarbons. Since the objective was to remove as much organically combined oxygen as possible the most interesting peaks for this study were: alcohols at 3550-3200 $cm^{-1}$ (O-H stretching) and above all carboxylic groups at 1780-1630 $cm^{-1}$ (C=O stretching).

**Table 1. Properties of gasification tar**

| Elemental analysis (on wet basis) | Weight percent | GC analysis | *Mole % of carbon* |
|---|---|---|---|
| C | 64.46 | Gasoline | ~0 |
| H | 7.21 | Kerosene | 11.5 |
| N | ~0 | Gas oil | 61.0 |
| O (by difference) | 28.33 | Residue. 369°C+ | 27.5 |

**Hydrodeoxygenation of gasification tar by catalytic hydrotreatment.** The first hydrotreating run was performed at high temperature (370°C) and pressure (10.0 MPa). The reactor was quickly blocked with coke and therefore it was confirmed that the tar must be pre-stabilized to be able to treat it at temperatures of about 400°C. In the last run the temperature and pressure were set to 300°C and 11.0 MPa. Then the reactor bed was also blocked by coke. Therefore the pre-Hydroprocessing of temperature of the tar must be in the temperature interval 200-300°C in similar way as for bio-oil produced by flash pyrolysis (1). The elemental analysis of untreated tar showed that it contained 28.3-weight percent oxygen, including the oxygen atoms in water. In Fig. 1 the elemental analyses show that the oxygen content of the tar clearly decreased with increasing hydrotreating temperature, as expected. The explanation for this result is that the higher the temperature the higher HDO reaction rates. The oxygen content decreased from 28.3 weight percent to 24.4% at the 7.0 MPa pressure level and to 21.6% at the 11.0 MPa pressure level when the temperature was increased from 200 to 280°C. It might seem like a small reduction of oxygen-containing compounds in the tar. But one must remember that the most reactive species have been deoxygenated. The influence of pressure on the HDO of tar, see the results from the elemental analyses in Fig. 1 was that the oxygen content decreased with increasing pressure. This is logical since the higher the hydrogen gas pressure the higher the concentration of active hydrogen atoms on the surface of the catalyst, which in turn leads to higher HDO reaction rates. The dependence of the pressure is not as strong as the temperature dependence.

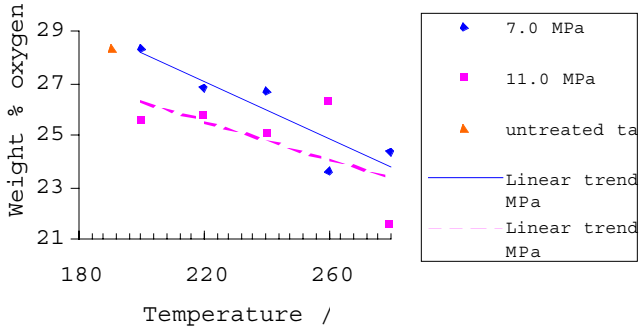


**Figure 1.** Elemental analysis: Effect of temperature on the oxygen content in hydrotreated tar. LHSV: 2.2 ± 0.3 $h^{-1}$.

At the lower pressure 7 MPa the same results were received as for the 11 MPa case. In Fig. 2 the carbonylic peaks in

the FT-IR spectra for untreated tar and hydrotreated tar at 7 MPa is zoomed in. It is clearly seen that the carbonylic absorption decreases with increasing hydrotreating temperature. Since the carbonylic absorption is a measure of the concentration of carbonylic compounds in the tar it is concluded that amount of C=O groups decrease with increasing temperature. For hydroprocessing at 11 MPa the results were similar.

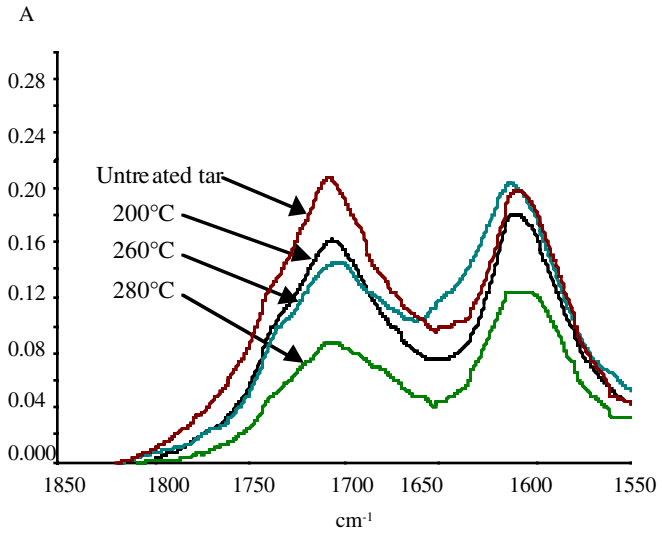


**Figure 2**.Comparison of FT-IR spectra for untreated tar and hydrotreated tar. Conditions: 7.0 MPa, LHSV= 2.2 ± 0.3 $h^{-1}$.

In the beginning of the test series a run with the following settings was performed: 10.0 MPa; 200°C; LHSV= 4.5 $h^{-1}$. To examine if the catalyst was deactivated during the experiments, a run with approximately the same hydrotreating conditions as above was carried out at the end of the test series: 10.0 MPa; 200°C; LHSV= 4.6 $h^{-1}$. The FT-IR analysis showed that the carbonylic peak heights of the two samples were 0.1995 and 0.1997 Absorbance units, respectively. Therefore approximately no deactivation of the catalyst could be indicated from the FT-IR analyses. Total time on tar stream was 42 hrs. When hydroprocessing tar from high-pressure liquefaction Gevert (5) found that the deactivation was quick during the first hours and leveled out to be constant. The same behavior is found here.

The results from the GC analyses in Fig. 3 show that the fraction of compounds with relatively low boiling points increase on the expense of compounds with high boiling points when the gasification tar was hydrotreated. This result is general for all this result is general for all hydroprocessing conditions analyzed. The explanation is that when the oxygen-containing compounds become hydrodeoxygenated the effect of hydrogen bonding and dipole-dipole interactions will decrease, which in turn means that the boiling points of hydrodeoxygenated compounds will be lowered. It is also interesting that the kerosene fraction increases from ~10 to ~20 mole percent already at 200°C, since the definite aim with this project is to produce aviation fuel from biomass. One possible reason to why the effects of LHSV and pressure from the FT-IR analyses were inconclusive could be that these effects only were studied at 200°C. At such mild conditions very few HDO reactions occur and it is therefore hard to say in what way different parameters influence the result. However, high hydrogen gas pressure and high LHSV counteracts coke formation and in that way the catalyst lifetime can be prolonged. The optimum hydrotreating condition for hydrodeoxygenation of the tar was thereby found to be 280°C, 11.0 MPa and LHSV=2.3 $h^{-1}$. Should the definite objective with this project fail, which is if it is difficult to produce aviation fuel components from tar formed in gasification of biomass with aid of hydrotreatment/hydrocracking, the product could be used to replace fuel oil. Then the value of the product would be lower but the environmental profits would remain.

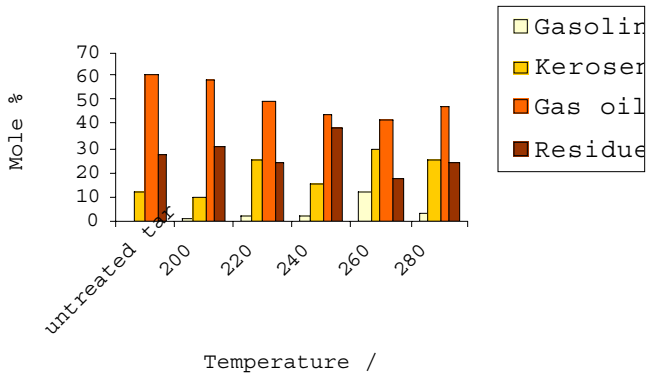


**Figure 3.** GC analysis: Effect of temperature on the yield of different fractions in hydrotreated tar and unhydrotreated tar. Pressure: 11.0 MPa, LHSV: 2.2 ± 0.3 $h^{-1}$

## Conclusions

Tar from gasification of biomass can be hydroprocessed.. The oxygen content of the tar decreased with increasing hydrotreating temperature. At temperatures >300°C the hydrotreating reactor was blocked with coke. Therefore it was concluded that the maximum (optimum) hydrotreating temperature was 280°C.The elemental analysis showed a tendency for decreasing oxygen with increasing pressure.The FT-IR analyses could not indicate any deactivation of the catalyst.Optimum hydrotreating condition was found to be: 280°C; 11.0 MPa; LHSV = 2.3 $h^{-1}$.

**Acknowledgement.** The authors would like to thank Swedish National Board for Industrial and Technical Development (NUTEK) and CF's Environmental foundation for financial support, Long Feixiang for assistance with the hydrotreating apparatus and Anders Mårtensson for help with FT-IR analyses.

## References

(1) Baker, E.; Elliott, D. In: Soltes, E.J.; Milne, T.A. (Eds). *Pyrolysis oils from biomass: producing analysing and upgrading*; ACS 376, Washington, DC, 1988; pp. 228-240.

(2) Ying Zhong-Shu, Börje Gevert, Jan-Erik Otterstedt, Johan Sterte, Applied Catalysis A, 153 (1997), 69-82.

(3) Furimsky, E., *Catalysis reviews science and engineering*. **1983**, *25*, 421-458.

(4) Grange, P.; Ceteno, A.; Maggi, R.; Delmon, B. In: Bridgwater, A.V.; Hogan, E. (Eds). *Bio-oil production and utilization*, 1996; pp. 186-197

(5) Gevert, B. In Bridgewater A.V. (Ed). Advances in Thermo Chemical Biomass Conversion, Blackie, London, 1994, 1424-1431.

# Influence of thermal treatment conditions on transformation behavior of trace elements in coals

*Ruixia Guo, Jianli Yang, Baohua Li, Dongyan Liu, Zhenyu Liu*

State Key Laboratory of Coal Conversion, Institute of Coal Chemistry, Chinese Academy of Sciences, P.O. Box 165, Taiyuan, Shanxi 030001, P.R. China

## Introduction

Coal contains harmful elements of environmental concerns in ppm order, such as Na, K, Pb and Mn. Release of these elements from coal as vapor or fine particles during coal combustion causes severe problems to the turbine blades, human health and ecological environment [1-3]. Therefore, a full detailed understanding on the chemical and thermal stability of Na, K, Pb and Mn during coal processing is desirable in guiding their effective control prior to combustion.

Recently, many researchers have studied the forms of Na, K, Pb and Mn in coal and their fate during coal combustion [3-7]. However, the information on the transformation of the elements during pyrolysis is limited. The attempt was made in this paper is to understand the transformation of Na, K, Pb and Mn during thermal treatments under different conditions. The effects of the temperature, pressure, and atmosphere were investigated. The pyrolysis temperature was found to be the most influential factor for Na, K, Pb and Mn evolution.

## Experimental

**2.1 Coal sample**. Two Chinese coals, Shenhua and Yima, were used in this study. The coals were crushed and sieved to 0.16~0.27mm, and then dried under vacuum at 110°C with a nitrogen purge. The properties of the coals are given in Table 1.

**Table 1. Analysis of coal samples，wt%**

| Coal sample | Proximate analysis | | | Ultimate analysis，daf | | | | | Ash analysis | |
|---|---|---|---|---|---|---|---|---|---|---|
| | $V_{ad}$ | $A_d$ | M | C | H | N | S | $O^a$ | Si | Al |
| Shenhua | 30.71 | 6.61 | 0.51 | 63.77 | 3.81 | 0.79 | 0.57 | 31.06 | 27.8 | 5.9 |
| Yima | 30.24 | 15.79 | 0.79 | 58.88 | 2.94 | 0.65 | 1.94 | 35.62 | 30.1 | 10.0 |

**2.2 Apparatus and Procedure**. A schematic representation of experimental apparatus is shown in Fig 1. It consists mainly of a rotary furnace and a pyrolysis reactor. Prior to a reaction，about 5g of coal sample was placed at the top of the reactor. Then it was sealed and filled with a desired gas to a pressure of 0.1 MPa or 5.0 MPa. During these processes, the reactor was maintained at horizontal position. After heating up the reactor to a desired temperature, the furnace, along with the reactor, was quickly turned to vertical position to allow fast pyrolysis. After 2 minutes, the reactor was pulled out from the furnace and quenched in the cold water. Char was collected from the bottom of the reactor. Amount of gases produced was determined by the weight difference of the reactor with the samples before and after the reaction. Amount of tar produced was calculated by subtraction.

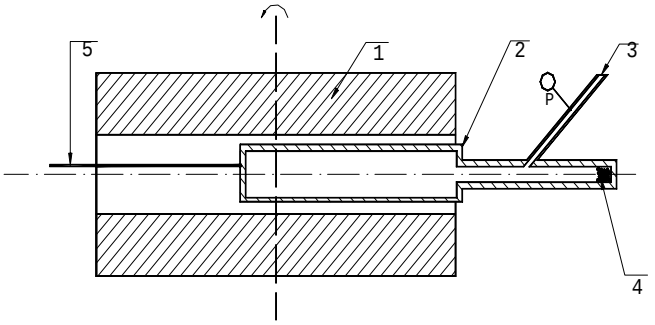


1 furnace, 2 reactor, 3 gas in and out, 4 coal sample 5 thermocouple
**Fig 1.** The schematic of high pressure closed fast pyrolysis apparatus

**2.3 Trace element analysis.** The forms of Pb and Mn contained in the coals were defined as the following: $H_2O$ solubles, HCl solubles and residues. Deionised water and aqueous solutions of 1N hydrochloric acid (HCl) were used for $H_2O$ solubles and HCl solubles seperation. The use of HCl removed acid soluble minerals such as calcite ($CaCO_3$), dolomite ($CaMg\ [CO_3]_2$), and siderite ($FeCO_3$). Clay (aluminosilicates), quartz ($SiO_2$), and pyrite ($FeS_2$) as residue remained in the solid. The content of Na, K, Pb and Mn in raw coal, char and solutions was measured by inductively coupled plasma – atomic emission spectroscopy (ICP-AES).

## Results and Discussion

**3.1 Release behavior of the elements in Shenhua and Yima coal.** Tables 2 and 3 show changes of Na, K, Pb and Mn content in chars with temperature during pyrolysis in a nitrogen atmosphere. Although contents of all the four elements decreased with increasing pyrolysis temperature, the initial emission temperature for Shenhua coal (400°C) is lower than that for Yima coal (600°C). The content of Na, K, Pb and Mn in chars varies with coal type. This indicates that the transformation of the elements is related to their forms in the coals and the environment around them. Larger amounts of Si, Al and S in Yima coal than those in Shenhua coal suggests that the elements in Yima coal may be existed as sulphate, aluminate and silicate of thermal stable forms. Due to high boiling point of these thermally stable compounds, their decomposition and transformation are difficult [6,7,11]. This resulted in the lower emission of the elements from Yima coal.

**Table 2. char yield (wt%) and the contents of elements for Shenhua coal（μg/g coal）**

| Temperature ℃ | Raw coal | 400 | 500 | 600 | 700 |
|---|---|---|---|---|---|
| Char yield | | 97.75 | 93.65 | 87.80 | 81.41 |
| Na | 1334.2 | 1334.2 | 1331.5 | 1328.9 | 1299.1 |
| K | 2963.1 | 2963.1 | 2963.1 | 2960.1 | 2927.5 |
| Pb | 13.1 | 13.1 | 13.1 | 12.5 | 11.8 |
| Mn | 41.8 | 41.8 | 41.8 | 41.7 | 40.8 |

**Table 3. char yield (wt%) and the contents of elements for Yima coal（μg/g coal）**

| Temperature ℃ | Raw coal | 400 | 500 | 600 | 700 |
|---|---|---|---|---|---|
| Char yield | | 93.61 | 91.41 | 86.70 | 81.00 |
| Na | 893.2 | 846.6 | 843.0 | 835.0 | 823.3 |
| K | 627.0 | 610.1 | 605.7 | 604.4 | 595.7 |
| Pb | 6.2 | 5.8 | 5.7 | 5.5 | 5.3 |
| Mn | 70.6 | 67.2 | 67.1 | 66.9 | 66.5 |

In order to further demonstrate the relationships between the behavior of the elements during heating and their chemical forms in the coals, the distribution of the forms for the elements in Yima and Shenhua coals were investigated. Results obtained for the elements Pb and Mn are presented in Table 4. It can be seen that Pb is predominantly present as $H_2O$ solubles and residues in Shenhua coal. However, the residues are the main forms of Pb in Yima coal. It is consistent with that Pb is often reported to be strongly associated with sulfur and Pb sulfides are $H_2O$ insoluble. In the experimental temperature range, residues are non-volatile compounds. This may lead to lower release of the elements from coals. $H_2O$ solubles of Pb were found in Shenhua coal but not in Yima coal. This results in the difference of initial emission temperature between two coals. However, percentage of Pb emitted (14.1%) up to 700°C is lower than that of $H_2O$ solubles (23%) based on total content in Shenhua coal. This suggests that the $H_2O$ solubles of Pb is not released to gas completely and partly converted into other forms during thermal treatment. In addition, Mn in both coals is distributed in all the three forms but $H_2O$ solubles fraction is negligible. This agrees with the non-volatile behavior of Mn.

**Table 4. Analysis of elements forms（μg/g coal）**

| solubles | Pb | | Mn | |
|---|---|---|---|---|
| | Shenhua | Yima | Shenhua | Yima |
| $H_2O$ | 1.7 | 0 | 1.2 | 0.1 |
| HCl | 0 | 1.1 | 57.8 | 0.3 |
| Residue | 4.6 | 11.8 | 11.6 | 40.3 |

**3.2 Influence of atmosphere.** Fig 2 (a) and (b) show the changes in content of Na, K, Pb and Mn in Shenhua coal during pyrolysis in $N_2$, $H_2$ and $CO_2$ atmospheres. Among the three atmospheres, $H_2$ results in the least elements retention and $CO_2$ the highest elements retention. The polymerization between siliceous char and volatile compounds is favorable in oxidizing atmosphere [8]. This may transform volatile compounds of Na, K, Pb and Mn into thermally stable compounds. In contrast, the high yield of volatile compounds (gas +tar) under $H_2$ (shown in Fig 3) increases the emission of the elements by transferring thermally stable compounds into low boiling point of compounds (such as chloride) [9]. As a result, $H_2$ and $CO_2$ resulted in obvious distinction on emission of the four elements.

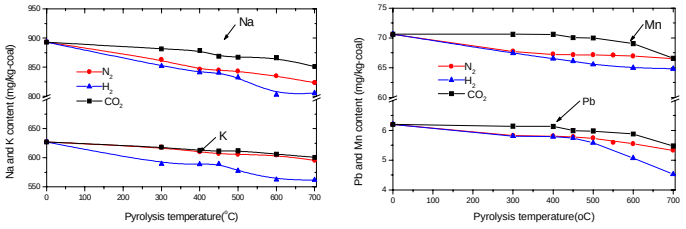


a b

**Fig 2.**The effect of atmosphere on evolve of elements in Shenhua coal
a：The effect on Na and K b：The effect on Pb and Mn

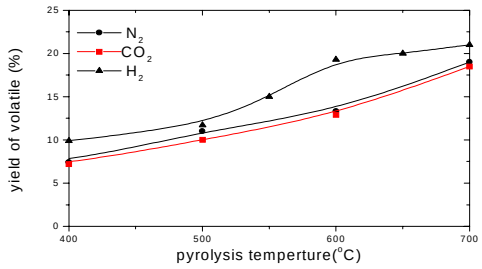


**Fig 3.** Yield of volatile for Shenhua coal during pyrolysis at 0.1MPa

**3.3 Influence of pressure.** The effects of pressure on the retention of Na, K, Pb and Mn in Shenhua coal during pyrolysis were given in Fig 4. Although lesser amounts of the elements were released at 5MPa than at 0.1MPa, the effect of pressure is small. Two important steps may affect the release of the elements: breaking of chemical bonds and transfer of the volatiles from the coal pore to the gas phase. Generally speaking, the former is not sensitive to the pressure, but the latter is affected by the pressure. The higher pressure restrains the transfer of volatile compounds from the pore of coal and increases the possibility of the element retention in the char. The thermodynamic analysis also confirmed this [10].

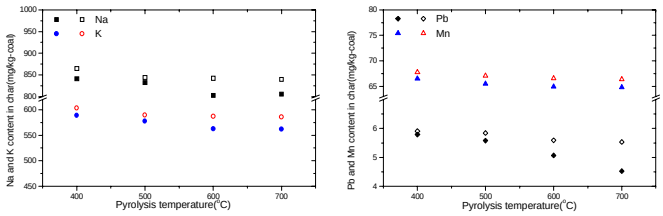


a b

**Fig 4**. The effects of temperature and pressure on evolve of elements for Shenhua coal in $H_2$: Filled symbol, 0.1MPa; Open symbol：5Mpa.
a: The effect on Na and K; b: The effect on Pb and Mn

## Conclusions

The effects of atmosphere, pressure and temperature on trace elements release behavior during thermal treatment were investigated. The elements studied are Na, K, Pb, and Mn. The order of atmosphere influence on the emission of the elements is H2> N2> $CO_2$. Although the effect of pressure is not significant, the higher pressure results in the lesser element emission. The emission of the four elements is mainly dependent on temperature and their forms in coal.

**Acknowledgement.** The authors gratefully acknowledge the financial support from the Special Founds for Major State Basic Research Project, the Chinese Academy of Sciences, and the Natural Science Foundation of China.

## References

(1). Manzoori, A. R.; Pradeep, K.; and Agarwal. *Fuel,* **1992**, *71* (5), 513.
(2). Peterson, J. R.; Lucke, V. H. *Combustion*, **1979**, *50* (7), 29.
(3). Feng, X.B.; Ni, J.Y.; Hong, Y.T.; Zhu, J.M.; Zhou, B.; Wang, Y. *Environmental Chemistry*, **1998**, *17* (2), 148.
(4). Helble, J.J. *Fuel Processing Technology*, **1994**, 39(1), 159
(5). John Hodges, N. D.; and Richards, G. *Fuel,* **1989,** *68*(1), 440.
(6). Han, C.l.; Zhang, J.; Liu, K.L.; Xu, Y.Q. *Journal of fuel chemistry and technology*, **1999,** *27*(6), 575.
(7). Huang, W.H.; and Yang, Q. *Geological Science and technology information,* **1999**, *18*(1), 71.
(8). Zhang, J.; Han, C.L.; and Liu, K.L. *Journal of Engineering for Thermal Energy and Power,* **1999**, *14*(2), 83.
(9). Enders, M.; Wilenborg, W.; Albrecht, J.; Putnis, A *Fuel Processing Technology,* **2000**, *68*(1), 57.
(10) Wang, X.F.; Sun, X.B.; and Li, M. *Coal Conversion*, **1999**, *22*(1), 58.
(11). Sugawara, K.; Inoue, H.; Enda, Y.; Sugawara, T.; Shirai, M.In *The 7th China-Japan Symposium on Coal and $C_1$ Chemistry Proceedings*; P.R.China, 2001; pp.367-370

# NITROGEN AND SULFUR RELEASE DURING HIGH TEMPERATURE PYROLYSIS OF COALS

*Naoto Tsubouchi and Yasuo Ohtsuka*

Institute of Multidisciplinary Research for Advanced Materials
Tohoku University
Katahira, Aoba-ku, Sendai 980-8577, Japan

## Introduction

The fate of the nitrogen and sulfur in coal during pyrolysis has been studied extensively with different reactors under various conditions[1-5], since it is related with $NO_x$ and $SO_x$ emissions in the subsequent combustion process. However, most of researchers have paid no attention to the release of these heteroatoms from char after devolatilization. There have been only a few papers on this topic so far[6-8].

It is of interest to make clear what factors can control such behavior during high temperature pyrolysis. The present work focuses on examining the influences of some factors on the nitrogen and sulfur release during coal pyrolysis at high temperatures of ≥ 1000°C, and on elucidating possible mechanisms.

## Experimental

**Coal Samples.** Ten coals with different ranks from different countries were used in this work. All the samples were air-dried at room temperature, ground and sieved to coal particles with size fraction of 150-250 μm. Their carbon, nitrogen, and sulfur contents ranged from 66 to 80 wt%, 0.9 to 2.0 wt%, 0.1 to 1.3 wt% on a dry ash-free basis, respectively.

Ca catalyst was loaded on the coal by using a saturated aqueous solution of $Ca(OH)_2$ in a rotary evaporator at room temperature[9]. The Ca content in the dried sample was 3 wt%.

**Pyrolysis.** Pyrolysis runs were carried out with a fixed bed quartz reactor[4], except for the use of a free-fall type quartz pyrolyzer under rapid heating conditions ($10^4$-$10^5$°C/s). After precautions against leakage, about 0.5 g of the sample was heated in a stream of high purity He (>99.9999%) at 400°C/min up to 1000°C-1350°C, soaked for 2 min, and then quenched to room temperature.

**Nitrogen and Sulfur Analysis.** Pyrolysis products were separated into gas, tar, and char in the same manner as described elsewhere[4]. $N_2$ in the gas was detected with a micro gas chromatograph, and the HCN and $NH_3$ were analyzed with a FT-IR equipped with a long-path gas cell. The nitrogen in the tar (tar-N) or in the char (char-N) was determined with conventional combustion-type elemental analyzers. $H_2S$ was analyzed by the Gastec standard tube. Yield of each nitrogen species or $H_2S$ is expressed in percent of total nitrogen or sulfur in feed coal, respectively.

**Char Characterization.** The XRD measurements of samples after pyrolysis were carried out with Ni-filtered Cu-Kα radiation (40kV, 30mA) to clarify crystalline forms and dispersion states of inherent minerals and added Ca. The average crystalline size of CaO was calculated by the Debye-Scherrer method.

## Results and Discussion

**Pyrolysis Temperature.** When the changes in yields of N-containing products between 1000°C and 1350°C were examined with all the coals used, $N_2$ was the dominant species and the yield increased almost linearly with increasing temperature with a corresponding decrease in char-N. On the other hand, yields of volatile-N (tar-N, HCN, and $NH_3$) were almost unchanged.

The increase in $N_2$ yield between 1000°C and 1350°C is plotted as a function of the decrease in char-N yield in **Figure 1**. There was a strong reverse correlation between $N_2$ and char-N, though some data were scattered at a larger extent of the decreased yield of char-N. The N/C ratios in the 1200°C and 1350°C chars, normalized to that in the 1000°C char, were lower at a higher temperature, irrespective of coal type. Thus, these observations point out that the $N_2$ increased arises mostly from char-N after devolatilization.

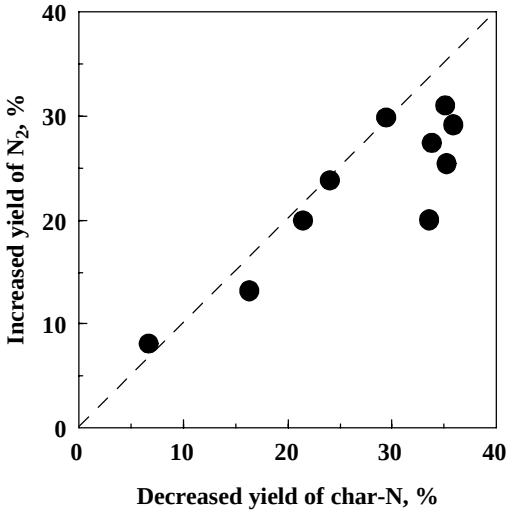


**Figure 1.** Relationship between $N_2$ and char-N.

Typical examples of $H_2S$ release between 1000°C and 1350°C are illustrated in **Figure 2**, where $H_2S$ yield is given for AD, LP, and TG coals. The yield increased with increasing temperature, and the increment depended on coal type. Although recent XPS and XANES studies have shown a clear trend of a larger proportion of thiophenic sulfur at a higher carbon content in coal[10], the increase in $H_2S$ yield observed between 1000°C and 1350°C was almost independent of coal rank. It is suggested that $H_2S$ formation under such conditions can not be correlated with the distribution of sulfur functional groups in coal.

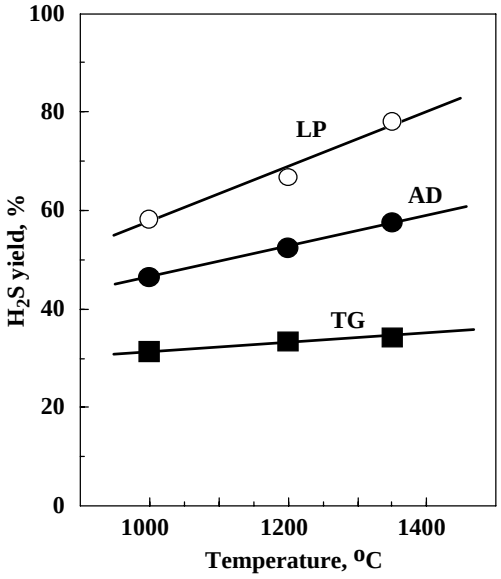


**Figure 2.** Temperature dependence of $H_2S$ yield.

**Solid Residence Time.** The dependence of yields of $N_2$ and $H_2S$ for AD coal on solid residence time at 1300°C is illustrated in **Figure 3**, where heating rate is $10^4$-$10^5$°C/s. Weight loss was almost unchanged with the time. Volatile matter in the present rapid pyrolysis was the same as or higher than that from proximate analysis, indicating complete release of volatile matter.

As is seen in **Figure 3**, a small amount of $N_2$ was observed at time of 0 s. The yield increased with increasing time and reached 37% at 120 s. On the other hand, char-N decreased with time, as expected. $H_2S$ showed almost the same time dependence as $N_2$, and $H_2S$ yield increased considerably from 38% at 0 s to 82% at 120 s.

**Figure 3** also shows the H/C ratio in the char after pyrolysis at time of 30 s or 120 s, normalized to that at 0 s. The ratio was smaller at a longer time. There was a reverse correlation between the decrease in H/C and formation of $N_2$ or $H_2S$. Since the decrease means the occurrence of aromatization reactions of char, it is likely that the formation of $N_2$ and $H_2S$ proceeds in the process of carbon crystallization.

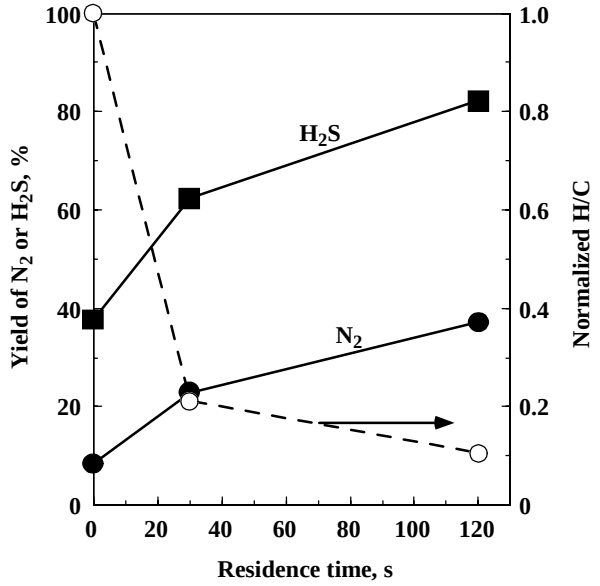


**Figure 3.** Effect of solid residence time on normalized H/C and yields of $N_2$ and $H_2S$ under rapid heating conditions.

**Calcium Addition. Table 1** shows the effect of Ca addition on the changes in yields of $N_2$, char-N, and $H_2S$ between 1000°C and 1350°C. The $Ca^{2+}$ ions added on AB and AD coals enhanced $N_2$ yield at high temperatures of ≥ 1000°C, but decreased char-N yield. The Ca on AD coal catalyzed $N_2$ formation more remarkably. This would be ascribed to the difference in the content of inherent Ca between both coals, that is, 1.8 wt%Ca for AB and 0.2 wt%Ca for AD, since the Ca added to a low rank coal with the higher content does not work efficiently. No changes in $H_2S$ yield for AB and AD coals by Ca addition were observed. In other words, the Ca suppressed $H_2S$ formation.

**Table 1. Effect of Ca Addition on formation of $N_2$ and $H_2S$**

| Coal | Ca loading (%) | Change in yield between 1000°C-1350°C (%) | | |
|---|---|---|---|---|
| | | $N_2$ | char-N | $H_2S$ |
| AB | 0 | +13 | -14 | +4 |
| AB | 3 | +15 | -16 | ±0 |
| AD | 0 | +27 | -32 | +11 |
| AD | 3 | +32 | -35 | ±0 |

The XRD measurements after pyrolysis revealed that the Ca existed predominantly as CaO with the average size of 15-30 nm in the 1000°C chars derived from Ca-loaded AB and AD coals and promoted carbon crystallization at high temperatures above 1000°C. When temperature was raised to 1350°C, the sizes increased slightly. Thus, the reaction between CaO particles and char-N may occur in the process of carbon crystallization. The small peaks of CaS were also observed. These observations indicate that the highly dispersed CaO catalyzes efficiently conversion reactions of char-N to $N_2$ at solid phase, and captures $H_2S$ evolved and/or reacts organic sulfur in the char.

A small XRD peak of CaO was also detectable in the chars from AB coal, though it was not observed for AD coal because probably of low content of inherent Ca. Therefore, the mineral-derived CaO can catalyze carbon crystallization, as observed in **Figure 3**. It is likely that $N_2$ formation from char-N and sulfur capture by CaO occur through the same mechanism as in the pyrolysis of Ca-loaded coal.

## Conclusions

To make clear nitrogen and sulfur release from char after devolatilization, ten coals have been pyrolyzed at high temperatures of ≥ 1000°C with both a fixed bed reactor and a free fall type reactor. Yields of $N_2$ and $H_2S$ increase with increasing temperature and solid residence time, whereas char-N decreases. The addition of 3 wt%Ca to low rank coals enhances $N_2$, whereas it decreases yields of char-N and $H_2S$. The Ca is transformed to fine particles of CaO, which catalyzes carbon crystallization. CaO particles may not only promote $N_2$ formation through solid phase reactions of char-N but undergo sulfur capture reactions.


## Acknowledgment

This work was supported in part by the Basic Research Associate for Innovative Coal Utilization (BRAIN-C) Program, sponsored by the New Energy and Industrial Development Organization (NEDO), Japan. The authors gratefully acknowledge Ms. Hazuki Satake for her assistance in carrying out experiments.


## References


1. Solomon, P. R., Colket, M. B., *Fuel* 1978, **57**, 749-755.
2. Chen, J. C., Castagnoli, C., Niksa, S., *Energy Fuels* 1992, **6**, 264-271.
3. Bassilakis, R., Zhao, Y., Solomos, P. R., Serio, M. A., *Energy Fuels* 1993, 7, 710-720.
4. Wu, Z., Ohtsuka, Y., *Energy Fuels* 1997, **11**, 477-482.
5. Sugawara, T., Sugawara, K., Nishiyama, Y., Sholes, M. A., *Fuel* 1991, **70**, 1091.
6. Tsubouchi, N., Ohshima, Y., Xu, C., Ohtsuka, Y., *Energy Fuels* 2001, **15**, 158-162.
7. Tsubouchi, N., Ohtsuka, Y., *Fuel*, in press.
8. Garcia-Labiano, F., Hampartsoumian, E., Williams, A., *Fuel* 1995, **7**, 1072-1079.
9. Ohtsuka, Y., Asami, K., *Catal. Today* 1997, **39**, 111-125.
10. George, G. N., Gorbaty, M. L., Kelemen, S. R., Sansone, M., *Energy Fuels* 1991, **5**, 93-97.

# NOVEL METHOD TO SYNTHESIZE CARBON MOLECULAR SIEVES WITH PETROLEUM COKES

*Ya LIU, Zi-Feng YAN* *

*State Key Laboratory for Heavy Oil Processing,*
*Key Laboratory of Catalysis, CNPC,*
*University of Petroleum, Dongying 257061, P R China*

## Introduction

Since Emmet found carbon molecular sieves (CMS) in 1948, various starting materials, such as coal, polymer, nuts shell and so on, have been used to synthesize CMS. Generally, the preparation process consists of two steps as followed:

(1) Prepare carbon precursor with initial pore system by carbonization or activation.

(2) Modify the pore texture of precursor by carbon deposition of organic substance to satisfy different separation[1].

Petroleum cokes, especially ordinary cokes, are the main waste residue of refinery and have not been made full use of so far. Petroleum cokes contain high carbon content and low ash content, which are expected to be the potential carbon resources. Developing the application field of petroleum cokes is favorable to both of environment and economy.

By now, there are many reports concerning the preparation of high surface activated carbon from petroleum cokes. What we now are interested in is how to control the pore texture of the porous carbon for different purpose. In this paper, petroleum cokes were used as starting material to prepare microporous carbon with sieving ability and the product has been tentatively applied in air separation.

## Experimental

**Preparation of carbon precursor.** The petroleum cokes were crashed to particle of 20~40 mesh and then impregnated in concentrated KOH aqueous solution in which the weight ratio of KOH to cokes was 1.5. The mixture was dried at 373 K in drying oven for several hours to form slurry and then moved into the reactor to activate thermally. In nitrogen atmosphere, the sample was heated at the rate of 10 K/min to a final temperature (1053~1123 K) and held isothermally for a period of time (60~120 min). Finally, the sample was cooled in nitrogen, washed to pH~7 and dried.

**Modification of pore texture.** The precursor was placed into tubular flowing reactor and was heated to 1053 K in nitrogen atmosphere and held isothermally for 60 min to get rid of surface functional groups from precursor. Afterward, the reactor was cooled to a certain pyrolysis temperature and then the hydrocarbon stream was introduced. The precursor was exposed to the hydrocarbon for a specified period. Following this treatment, the sample was degassed in nitrogen at the same temperature for 60 min and then cooled to ambient condition.[2]

**Characterization of pore texture.** The adsorption of nitrogen at 77 K was performed on Micromeritics ASAP2010 instrument to characterize the pore texture. Data of micropore and transitional pore were calculated by H-K and BJH method respectively.

**Evaluation of sieving ability.** Air separation was performed on small-scale single volume PSA apparatus to evaluate the sieving ability of the product. The size of the adsorption volume is 3.5×300 mm and the weight of adsorbent was about 1 g. The operating procedures were as followed:

(1) Vacuumize for 3min.

(2) Introduce air and perform adsorption at ambient pressure

(3) Repeat the above two steps for several times to attain the average result

## Result and discussion

**Influence of activation condition on the pore texture of carbon precursor. Effect of activation time.** Fig.1 and 2 showed that micropore diameter of precursor increases initially and then decreases along with activation time while the micropore volume decreases at first and then increases with activation time. Furthermore, the activation time correspondent with the minimum micropore volume and the largest micropore diameter is coincidently in agreement. It was speculated that the micropore forms initially and then activation reagents gradually diffuse into the nanopore system and continue erode and enlarge the wall of the micropore during the activation, which leads to the increase of micropore volume and size. Meanwhile, some micropores become so larger that they could turn into transitional pore even macropores or connect with each other to become larger, so the micropore volume decreases and micropore becomes small. However, the subsequent corruption of the wall of the larger pores results in the new micropore with smaller size, which may increase micropore volume. The other reason why micropore

*Corresponding author. E-mail: zfyancat@hdpu.edu.cn

diameter decreased may be the fragment of organic substance from cokes blocked the micropore.

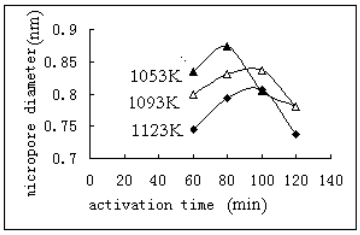


**Fig. 1** The effect of activation time on the micropore size

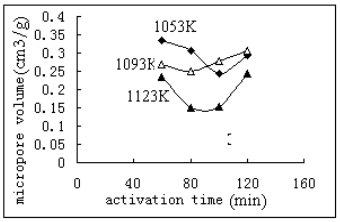


**Fig. 2** The effect of activation time on the micropore volume

**Effect of activation temperature**. Fig.3 and 4 illustrated that both of micropore diameter and micropore volume increased initially and then decreased as temperature rose. However, the culmination temperature is not the same. It means that higher activation temperature accelerated the process of nanopore or micropore generation, but excessive high temperature resulted in the shrinkage of the micropore. The key to synthesize ideal precursor is to optimize activation temperature.

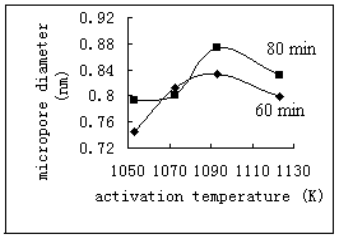


**Fig. 3** The effect of activation temperature on the micropore size

**Nanopore structure.** Sample AC-3# bears abundant and smaller size micropore with rather narrower nanopore distribution (Table 1), which was the selected carbon precursor that subjected to further treatment. It means that thermal activation assisted by KOH is feasible to synthesize optimum carbon precursor with initial nanopore structure. Of course, the activation condition must be seriously controlled.

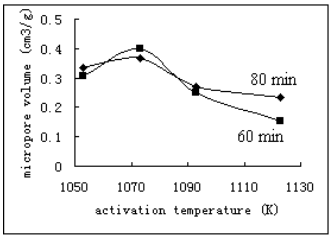


**Fig. 4** Effect of activation temperature on the micropore volume

**Modification of the textural properties by carbon deposition. Pyrolysis of LPG**. While liquefied petroleum gas was applied as nanopore modifer of precursor, the operating condition, such as the concentration of LPG, the pyrolysis temperature and pyrolysis time were extensively investigated, unfortunately, it was in vain. The modified product showed very weak air separation ability. Meanwhile, it was found that the BET surface area and pore volume decrease with the increase of pyrolysis temperature or pyrolysis time. Of interests were that the loss of micropore volume is always more severe than that of transitional pore (illustrated by Fig. 5) and that micropore diameter became larger with the loss of micro pore volume after carbon deposition (illustrated by Fig. 6).

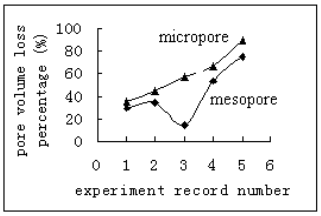


**Fig. 5** Profile of pore volume loss percentage

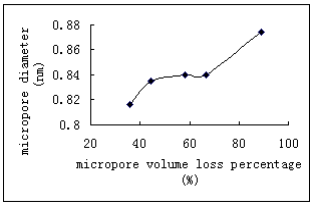


**Fig. 6** Relation between micropore diameter and volume loss

According to a widely accepted pore texture modal, porous carbon bears macropore, transitional pore and micro pore. Transitional pore is branched off from macropore and micropore is branched off from transitional pore. Macropore and transitional pore serve as a passage of gas molecular and micropore practices separation in deed. Gas-solid heterogeneous reaction such as carbon deposition consists of external diffusion, internal diffusion,

adsorption, surface reaction, desorption, internal diffusion and external diffusion. Simultaneously, the homogeneous pyrolysis of hydrocarbon must be taken into account. So where the carbon deposition will occur depends on the relative speed of each step.[3] Therefore it was speculated that hydrocarbon molecular (or the product of homogenous pyrolysis) could easily enter the transitional and micropore. The carbon from pyrolysis either filled the micro pore or congested the opening of the micro pore located on the wall of the transitional pore. Moreover carbon molecular perhaps occurred on the wall of transitional pore, diminished the size of the pore and formed new micropore. Because smaller micropore tends to be blocked and the size of newly formed micropore is larger, so in general the average diameter of micropore increases.

**Pyrolysis of butene.** The available results were indicated in Table 2. Compared with the pyrolysis of LPG, butene is rather feasible to modify the nanopore of carbon molecular sieve samples. The nanoporous CMS sample indicated the favorable air separation ability. It means that the complexity of LPG constitute and too lighter lead to be difficult to control the pyrolysis reation.

The air separation performance of a commercial CMS was compared on the same apparatus under the same operating conditions. The concentration of nitrogen was 92.751%. We will also investigate the influences of butene concentration, flow velocity, cracking time and temperature.

**Effect of carbon precursor.** Another carbon precursor (AC-7, showed in Table 1) was used to repeat the above experiment of butene. The product exhibited no air separation ability. It means that the nanopore properties of precursor is very important to do subsequent modification of nanopore.

**Conclusions**

(1) Petroleum cokes were feasible to be the starting material for producing carbon molecular sieves.

(2) Nanoporous carbon precursor could be synthesized by thermal activation assisted by KOH activator.

(2) During the carbon deposition procedure, the kind of hydrocarbon and the pore texture of precursor are critical. Butene might be the optimum feed to modify the nanopore structure of CMS samples.

(3) The theory concerning the gas-solid heterogeneous reaction should be tentatively introduced to elucidate carbon deposition mechanism.

**Acknowledgement.** This program was financially supported by Key Teacher Foundation, Department of Education, China. Prof. Qian L., Song C.-M. And Dr. Liu X.-M., who give many beneficial discussions on this paper, were acknowledged.

**Reference**

(1) Shaoping, Xu; Shucai, Guo. *Coal Conversion,1995,18(3),43*

(2) S.K.Verma; P.L.Walker,Jr. Carbon, 1993, 31(7), 1203

(3) M.M.A.Fereitas; J.L.Figueiredo. Fuel, 2001, 80,1

**Table 1. The Properties of Carbon Precursor**

| | Activation temp. (K) | Activation time (min) | Micro-pore diameter (nm) | Micro-pore Volume ($cm^3/g$) | Micropore volume/ total pore volume (%) |
|---|---|---|---|---|---|
| AC-3 | 1053 | 120 | 0.74 | 0.29 | 80.78 |
| AC-7 | 1123 | 60 | 0.80 | 0.23 | 76.73 |

**Table 2. The Carbon Deposition of Butene**

| Sample | Cracking temperature (K) | Concentration of nitrogen (vol.%) |
|---|---|---|
| CD-1 | 973 | 83.31 |
| CD-2 | 993 | 84.67 |
| CD-3 | 1013 | 83.52 |
| CD-4 | 1033 | 83.79 |
| Commercial CMS | ---- | 92.75 |

# PYROLYSIS YIELDS OF COAL TAR PITCHES: EFFECT OF POLYMERIZATION ADDITIVES

*M. Mercedes Maroto-Valer, Yinzhi Zhang, Brandon N. Shaffer and John M. Andrésen*

Department of Energy and Geo-Environmental Engineering and The Energy Institute, The Pennsylvania State University, University Park, PA 16802.

## Introduction

The pyrolysis of coal tar pitches is associated with the emission of hazardous and carcinogenic polyaromatic hydrocarbons (PAHs) resulting in strong environmental and commercial challenges from the carbon industry (1). In order to prevent the shortcomings of the weight loss of coal tar pitches during pyrolysis, while optimizing their properties, a series of additives are routinely used to achieve high carbon yields upon baking or pyrolysis (2, 3). These additives typically include sulfur compounds that promote the polymerization of coal tar pitches and therefore increase the carbon yields. Although these sulfur additives effectively increase the carbon yields, they also evolve detrimental sulfur species upon baking. Accordingly, this work compares the pyrolysis yields of conventional sulfur additives as well as a series of alternative additives on basis of the pitch yield.

## Experimental

The coal tar pitch and calcined coke samples used for this study were supplied by Carbone of America. The thermogravimetical analysis (TGA) were carried out on a Perkin Elmer TGA-7 with a heating rate of 5°C/min from ambient up to 900°C, using about 10 mg of sample under a flow of $N_2$. The production of green carbon bodies was conducted following a protocol previously established by the investigators (4). The paste mix was heated to ~130°C and pressed into pellets to produce carbon bodies with dimensions of ~ 27mm in diameter and 15mm in height. The absolute densities of the pellets were measured by using a Quantachrome MVP-1 Multi Pycnometer and employing helium as density medium. The green bodies were baked in a closed system by placing them inside crucibles and covering them with calcined petroleum coke. The crucibles were then placed inside a muffle furnace and the baking program used was as follows: (1) 25-500°C at 10°C/hour; (2) 500-1075°C at 25°C/hour; and (3) held at 1075°C for 16 hours, providing an overall length of around 5 days for a completed baking and cooling cycle. Closed environments and slower baking programs have been previously reported to result in significant higher pitch yields and apparent and helium densities than those reported for open systems (5).

## Results and Discussion

**Comparison of pyrolysis pitch yield.** The thermal gravimetric profiles of the pitch alone and its mixtures with additives A1 and A2 are shown in Figure 1. The investigated pitch started losing weight at temperatures above 150°C and lost around 62 wt% during its carbonization at temperatures up to 850°C. When the pitch was mixed with different concentrations of the additive A1, the weight loss at 850°C was reduced, indicating an improvement in the solid yield, compared to that of the pitch alone. Furthermore, the pitch yield increased with the amount of additive at concentrations up to 10 wt% addition of A1 (3). The initial weight loss observed for the pitch/additive mixture was attributed to weight loss directly associated with the additive A1, as also indicated by the fact that the mixture with the highest additive content started losing weight at lower temperatures.

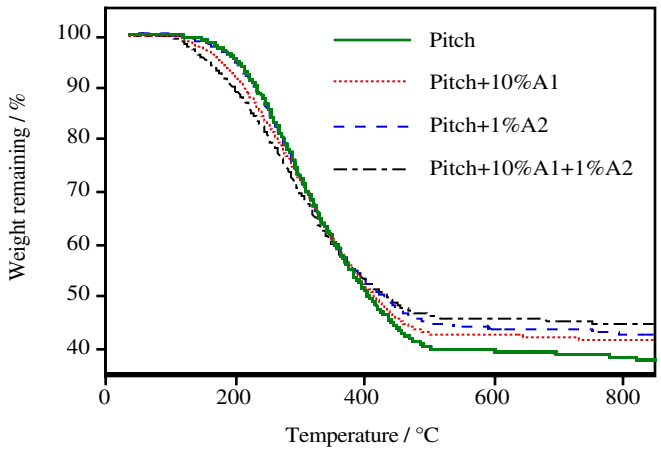


**Figure 1.** Comparison of the pyrolysis TGA traces for the coal tar pitch alone and mixed with additives A1 and A2.

A second additive A2 was also investigated and showed that when the pitch was mixed with only 1 wt% of A2, the weight loss at 850°C was reduced, indicating an improvement in the solid yield, compared to that of the pitch alone. Therefore, lower concentrations of additive A2 produced similar pitch yields to those observed at higher concentrations of additive A1. When the pitch is mixed with hybrid additives (10 wt% of A1 and 1 wt% of A2) the weight remaining at temperatures above 400°C is higher than when using only A1 or A2 (Figure 1). As previously observed for single additives, the pitch/additive A1+A2 mixture started to lose weight at temperatures lower than the pitch alone (120°C vs. 150°C) and presented larger weight loss than the pitch alone in the temperature range 120°C-300°C, due to weight loss directly associated with the additives (3). The pitch yields observed for the hybrid mixture were higher than those reported for the single additives, indicating that a possible synergistic effect takes place when adding both additives.

Sulfur additives, namely S1 and S2, were also tested to compare their performance with the alternative polymerization additives A1 and A2. When adding 1 wt% of S1, the pitch weight loss decreased from 62 wt% to around 58 wt% at 850°C. Similar pyrolysis pitch yield was reported when adding 1 wt% of A2, indicating that the additive A2 has similar performance in terms of pitch yield to S1. However, the mixture of pitch with sulfur additive S1 presents very similar weight loss profile to that of the pitch alone at temperatures <200°C, while the additives A1 and A2 presented higher weight loss in that temperature range. The pyrolysis pitch yields at 850°C of all the additives mixtures are compared in Figure 2. The alternative additives A1 and A2, have at least equal or superior performance in terms of pitch yields than conventional sulfur additives S1 and S2. Furthermore, the mixture of pitch with 10 wt% additive A1 presented higher pitch yield than the other mixtures, including those of the sulfur additives S1 and S2. The pitch yields observed for the hybrid mixture were higher than those reported for the sulfur additives. Finally, the pitch yields obtained from the thermogravimetric studies are generally low, due to the open system used as well as the high heating rates (5).

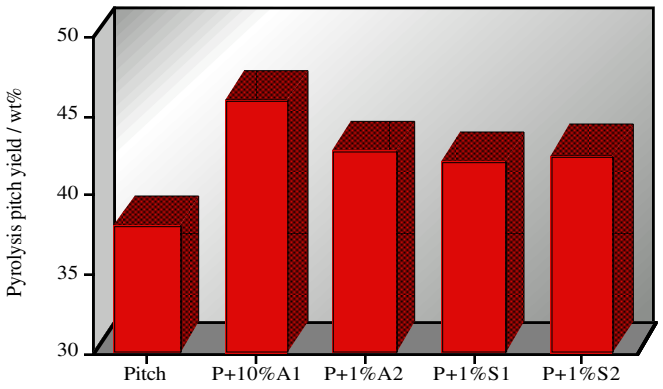


**Figure 2.** Pyrolysis pitch yields for the pitch alone and the mixtures with the different additives.

**Comparison of pyrolysis pitch baking yields for alternative additives and sulfur additives.** Carbon bodies were prepared using the alternative additives A1 and A2 as well as the sulfur additives S1 and S2 to compare their pitch yields. The green carbon bodies prepared with S1 and S2 contained seven different particle size coke fractions, while the green carbon bodies prepared with the A1 and A2 additives only contained two coke fractions. Table 1 shows that the apparent and helium densities of all the green carbon bodies prepared with the different additives were very similar, indicating that the additives did not have any impact in the density of the carbon body produced.

**Table 1. Apparent and helium densities for the green carbon bodies.**

| I. D. | Apparent Density g/cc | Helium Density g/cc |
|---|---|---|
| CB | 1.574 | 1.783 |
| CB-A1* | 1.762 | 1.829 |
| CB-A2* | 1.764 | 1.843 |
| CB-S1 | 1.683 | 1.791 |
| CB-S2 | 1.710 | 1.752 |

* Formulation comprises two coke fractions, while the other formulations comprise seven coke fractions.

Table 2 shows the pyrolysis pitch yields and the helium densities of the baked carbon bodies prepared with the additives A1, A2, S1 and S2. The baking temperature was 1075°C, as previously described. The helium densities of all the baked bodies are in the range 2.031-2.097g/cc (Table 2).

**Table 2. Pyrolysis pitch baking yields and helium densities for the baked carbon bodies.**

| I. D. | Baking Temperature °C | Pitch Yield % | Helium Density g/cc |
|---|---|---|---|
| CB-1075 | 1075 | 69.5 | 2.077 |
| CB-A1-1075* | 1075 | 73.4 | 2.097 |
| CB-A2-1075* | 1075 | 75.8 | 2.093 |
| CB-S1-1075 | 1075 | 72.7 | 2.057 |
| CB-S2-1075 | 1075 | 72.5 | 2.031 |

* Formulation comprises two coke fractions, while the other formulations comprise seven coke fractions.

Figure 3 shows the pyrolysis pitch baking yields of the carbon bodies. When using the A1 and A2 additives, the pyrolysis yields are slightly higher than the yields of the bodies prepared using the S1 and S2 sulfur additives. One caveat in this comparison is the different formulations used, where the carbon bodies prepared with the S1 and S2 sulfur additives contained seven different coke fractions, while the green carbon bodies prepared with the A1 and A2 additives only contained two coke fractions. Accordingly, further studies will be conducted to assess the effect of the coke formulation and also to investigate higher concentrations of S1 and S2 additives.

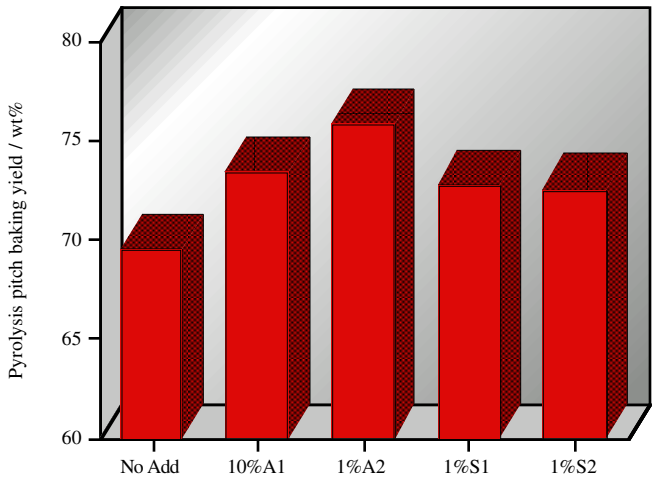


**Figure 3.** Pyrolysis pitch baking yields for the carbon bodies.

## Conclusions

There is a clear need to reduce the emissions of PAHs from coal tar pitches by improving the pyrolysis yield. This study has shown that all the polymerization additives tested thus far increase the pitch yields, with the highest pitch yields corresponding to the hybrid additives A1+A2. The polymerization additives tested, A1 and A2, present higher yields than the S1 and S2 sulfur additives tested. The helium and apparent densities of the green and baked carbon bodies are very similar, regardless of the type of additive used.

**Acknowledgements.** The authors would like to acknowledge the Carbon Research Center of The Pennsylvania State University for support.

## References

(1) Cirovic D.; Brereton R.G.; Walsh P.T., Ellwood J.A.; Scobbie E. *Analyst*, **1996**, 121(5), 575.
(2) Zhang, Y.; Maroto-Valer, M.M.; Andrésen, J., Proc. of Carbon'01, July 14-19, 2001, CD paper.
(3) Andrésen, J.M.; Zhang, Y.; Jensen, K.; Rusinko, F.J.; Schobert, H.H.; Prepr. Am. Chem. Soc. Div. Fuel Chem., 2001, 46(1), 292-293.
(4) Maroto-Valer, M.M.; Andrésen, J.M.; Andrésen, C.A; Battista, J.J., 1999 Int. Ash Utilization Symposium, 534-540.
(5) Maroto-Valer, M.M., Andrésen, J.M., and Zhang, Y., 2001, Carbon Research Center, Tech. Transfer Session Progress Report, The Pennsylvania State University, May, 2001.

# Ruthenium ion catalyzed oxidation as a tool for the characterization of pyrolysis non-volatile products

*Marco Antonio G. Teixeira, Maria Luísa A. Gonçalves, Rosana C. L. Pereira*

PETROBRAS R&D Center/Chemistry
Cidade Universitária, 21949-900, Rio de Janeiro, RJ, Brazil
marcoa@cenpes.petrobras.com.br

## Introduction

Processing high-density petroleum feeds, that are nowadays very important in the scenario of fossil fuel supplies, brings naturally the challenge of dealing with abundances of heavy ends and coke precursors. On the other hand, the optimization of refining facilities to deal with such feeds brings economical competitiveness, since these oils have low prices in the international market.

Studies on pyrolysis mechanisms are quite important under this aspect. Coking units, for example, which have traditionally been the second places among refining units, after FCC, may have their operation optimized with deeper knowledge on the pyrolysis mechanisms. Even the operation of FCC units, specially the ones processing distillation residua as part of their feed or its integrality, may take advantage of pyrolysis studies, since in these cases a meaningful portion of the coke formed in the reversible deactivation of the catalysts may come from thermal degradation of the feeds. In summary, as previouly stated by Speight (1), the key for optimization in the conversion of heavy residua lies on the understanding of coking phenomena, though the understanding of the main coke percursors, which are asphaltenes. In a previous study of thermal decomposition of asphaltenes, that author (2) had worked on the thermal decomposition of asphaltenes from 300 to 900ºC, and observed the occurrence of low molecular weight species in the volatile products. The most complex aromatic systems remain as coke, the non-volatile residue (45 % in weight).

Many efforts on the understanding of pyrolysis mechanisms can be found described in literature, and a main techinque for that is thermogravimetry, mainly if coupled to GC-MS; however, most of them are dedicated to the study of the volatile products formed (3-9). Of course those fractions are the most important ones from the economical point of view, since these are the ones that can be converted to valuable fuel products; nevertheless, the fact that completely established analytical approaches for the characterization of the coke formed do not exist is a major limitation to the study of this fraction, which is quite important to bring a full comprehensive analysis of pyrolysis phenomena.

This paper brings a novel approach for that aim. Ruthenium ion catalyzed oxidation (RICO) is employed to allow a better characterization of the coking process. That reagent allows selective oxidation of aromatic structures. $CO_2$ is the product of these oxidations in aromatic carbons. Alkyl side branches yield carboxylic acids, while naphtheno-aromatics and chains connecting two aromatic nuclei yield dicarboxylic acids. Condensed aromatics yield mainly dicarboxylic aromatic acids (*e. g.*, the main product of the oxidation of naphthalene is phthalic acid).

Since coke is basically constituted by aromatic nuclei with aliphatic branches, the relative yields and the distribution of products can be expected to be an indication of coke structure. This was confirmed in the present work. The application proposed was employed for the monitoration of the different structures of coke generated by the pyrolysis of asphaltenes at several decomposition temperatures.

So, conditions were proposed to execute the RICO reaction with coke. The strategy considered here is to employ this characterization scheme as a complimentary source of information to the study of volatile product formation, which can be monitored by some of the techniques mentioned above.

## Experimental Procedures and Results

For a perfect control of the conditions of pyrolysis of asphaltenes, a TG oven was employed. The collection of volatile material was achieved by passing the effluent gas stream into dichloromethane. Previous experiences employing TG-GC-MS showed that interface optimization can be necessary for that. The scope of this work did not aim the characterization of these products; that has been discussed elsewhere (10).

Asphaltenes from a Brazilian oil obtained by IP-143 were the material chosen to undergo pyrolysis . Table 1 shows the elemental analysis and aromaticity (ratio of the area of the envelope in the range of 160-100 ppm and total area of solid state $^{13}C$ NMR spectra) of those asphaltenes and cokes obtained after their pyrolysis at several temperatures.

**Table 1. Characterization of Asphaltenes Submitted to Pyrolysis and Cokes Obtained at Several Temperatures**

| Temperature (°C) | Coke (weight %) | %C | %H | % aromatic carbon | Atomic ratio (C/H) |
|---|---|---|---|---|---|
| -* | -* | 85.8 | 8.4 | 55.5 | 0.85 |
| 320 | 94 | 85.9 | 7.8 | 60.9 | 0.92 |
| 380 | 90 | 86.2 | 7.6 | 66.8 | 0.95 |
| 400 | 87 | 86.3 | 7.2 | 67.8 | 1.00 |
| 440 | 65 | 85.7 | 6.2 | 75.5 | 1.15 |
| 480 | 53 | 88.7 | 4.1 | 82.3 | 1.80 |
| 550 | 51 | 87.0 | 3.3 | 97.8 | 2.20 |
| 580 | 50 | 86.4 | 2.7 | 99.0 | 2.67 |

*original asphaltenes

The RICO reaction was performed using an adaptation from literature (11,12). The procedure consists of stirring, 150 mg of asphaltenes or pyrolysis residues obtained at each temperature, at 40ºC for 24 hours with $CCl_4$ (20 mL), $NaIO_4$ (3.4 mg), $H_2O$ (30 mL), acetonitrile (20 mL) and $RuCl_3.H_2O$ (7 mg).

The resulting two layers are separated and the organic phase, after being concentrated, was mixed with excess of ethereal diazomethane.

The ethereal solution was analyzed submitted by a gas chromatography/mass spectometry (GC/MS) for methyl ester analysis. Samples were injected with the previous addition of an internal standard in splitless mode using a 5%-phenyl 95%-methyl siloxane capillary column (30 m x 0.25 cm x 0.25 μm) and helium as carrier gas. Mass spectrometer was operated in electron impact ionization mode (70 eV) and scanned from 15 to 450 m/z.

As long as similar conditions were employed in all of the oxidation procedures, a comparison by the absorbance at the same wavenumber of the esters obtained after oxidation and reaction with diazomethane could be considered an indication of the relative yields. This was possible by doing equal dilutions of isolated materials after each reaction and recording the infrared spectra of the solutions.

Table 2 shows a comparison the ratios of the total responses of the esters of the cokes obtained at different temperatures to the

total responses of the esters obtained form the asphaltenes by GC/MS (total ion area with corrections were made using the areas of the internal standard) and infrared spectrophotometry (absorbances). These data cannot be taken as quantitative or strictly comparable ones, since it is well known that MS responses and infrared absortivities vary with the distribuiton of components in each sample, and the analyses refer to the reaction products, which are mixtures of different components depending on pyrolysis temperature. However, it can be seen that there are basically 3 groups into which the pyrolysis temperatures can be divided: before 380ºC there is no meaningful variation, while after 440ºC there are no more appreciable amounts of non polycondensed aromatic material. In fact, kinetic studies (10) show that the temperature in which pyrolysis has its maximum speed is 425°C.

**Table 2. Indications Of Relative Yields Of Esters From The Oxidation Of Cokes (Ratio To The Responses From Asphaltene Oxidation) By 2 Techniques**

| Temperature (°C) | Infrared | MS |
|---|---|---|
| 320 | 0,95 | 0,94 |
| 380 | 0,47 | 0,76 |
| 400 | 0,45 | 0,69 |
| 440 | 0,13 | 0,04 |
| 480 | 0,11 | 0,04 |
| 550 | n.r.* | 0,01 |
| 580 | n.r.* | n.r.* |

*negligible responses

Figure 1 summarizes the main classes of esters found by MS and shows the relative abundance of each of these classes, in terms of the ratios of their collective area in total ion chromatograms to the area of the internal standard (*raid*). It can be seen that linear chain esters are the most important ones in asphaltenes and in low temperature coke, indicating the abundance of linear aliphatic side chains in these samples.

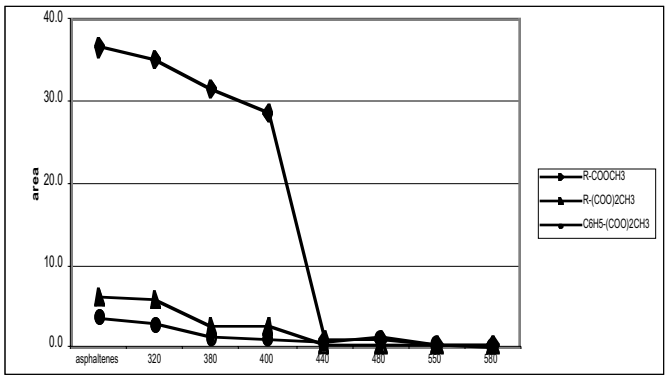


**Figure 1.** Yields of esters after RICO of cokes obtained by asphaltene pyrolysis at several temperatures

Figure 2 shows that, as a general tendency, the higher the number of carbons, the lower the temperature the side chains undergoes pyrolysis.

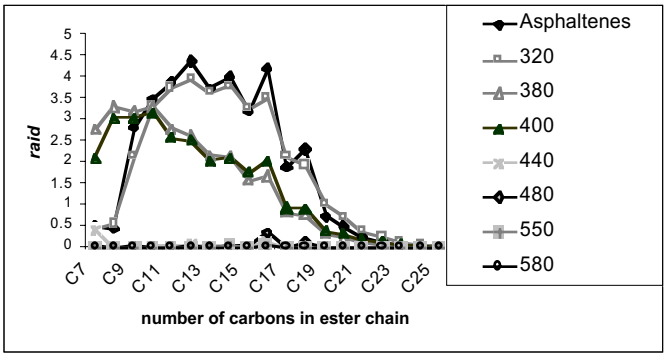


**Figure 2.** Distribution of monoesters after RICO of cokes obtained by asphaltene pyrolysis at several temperatures

## Conclusions

RICO followed by esterification of the oxidation products is a useful tool to the study of pyrolysis material (coke). It allowed some important inferences, about the fact that the profile of remaining components after heating asphaltenes dramatically changes in temperatures above 440°C, about the distribution of aliphatic chain lengths in cokes obtained at different temperatures, and about the tendency of ease of the alkyl groups bonded to aromatic nuclei to undergo pyrolysis according to the number of carbons in the chain. Future studies by the authors aim the integration of the data into a reasonable pyrolysis pathway.

## References


(1) Speight,, J. G., . Prepr. Pap. - Am. Chem. Soc., Div. Fuel Chem, **1994**, 39(2), 200.
(2) Speight, J.G., In Characterization of heavy crude oil and petroleum residue, Ed. Technip: Paris, 1984, pp.29-32.
(3) Wilhems, A., Larter, S.R., E Schulten, H.R., Org. Geochem., 20(7), **1993,** 1049.
(4) Skjevrak, I., Larter, S. Graas, G.V., Jones, M. Berger, E., Org. Geochem., **1993**, 22(3/5), 873.
(5) Eglinton,T.I., Larter, S.R., Boonmj.J., J. Anal. Appl. Pyr., **1991**, 20, 25.
(6) Jones, D.M., Douglas, A.G., Energy & Fuels, **1987**, 1, 468.
(7) Bestougeff, M.A., Guiochon, G., Jaqueé, J. Compt. Rend., **1962**, 254(2), 266.
(8) Nicksic, S.W., Jeffries-Harris, M. J., J. Inst. Petrol., **1968**, 54(532), 107.
(9) Calderon, J.L., Cotte, E., Rev. Tec. INTEVEP, **1983**,3(1), 69.
(10) Gonçalves, M. L. A., Teixeira, M. A. G., Pereira, R. C. L., Mercury, R. L. P., Matos, J. R., J. Therm. Anal. Cal., **2001**, 64, 697.
(11) Strausz, O.P., Mojelsky, T.W., Montgomery, D.S., Aostra J. Res.**,** **1985**, 2(2), 131
(12) Murata, S., U-Esaka, K., Ino-Eu, H. Nomura, M., Energy & Fuels**, 1994**, 8(6), 1379.255-274.

# SIMULTANEOUS COAL GASIFICATION AND $CO_2$ SEQUESTRATION USING A FLUIDIZED BED OF ACTIVATED SERPENTINE

*Zhong Tang, M. Mercedes Maroto-Valer, Yinzhi Zhang, Matthew E. Kuchta, John M. Andrésen and Scott A. Bair*

209 Academic Projects Building, The Energy Institute
The Pennsylvania State University, University Park, PA 16803

## Introduction

Coal has been the main energy supplier over a century and will continue being an important energy source in the 21st century. Unfortunately, all the coal utilization technologies used today, such as combustion and gasification, are inevitably associated with $CO_2$ emissions, and subsequently linked to the greenhouse effect and climate change by the public opinion. Therefore, the greatest challenge to achieve no environmental impact or zero emission in the 21st Century Energy Plant is probably the elimination of greenhouse gases emissions.[1]

Mineral carbonation, that involves the reaction of $CO_2$ with non-carbonate minerals, such as serpentine, to form stable mineral carbonates, has been lately proposed as a promising $CO_2$ sequestration technology due to the vast natural abundance of the raw minerals, the long term stability of the mineral carbonates formed, and the overall process being exothermic, and therefore, potentially economic viable.[2] Furthermore, mineral carbonation technologies could potentially provide a direct path to remove $CO_2$ when integrated with other systems, such as gasification processes. Using $CO_2$ sequestration as a part of the gasification process can be a highly efficient, environmental friendly and economical alternative to combustion technologies, since the volume of fuel gas in gasification is significantly lower than that of flue gas generated by combustion. In addition, the concentration of $CO_2$ is higher in fuel gas than in flue gas[3].

In the present study, a lab-scale fluidized bed gasification unit was used to investigate the effect of in-bed carbon dioxide removal during coal gasification using activated serpentine, which was produced by the novel active carbonation concept. [4]

## Experimental

**Char Samples.** For this study, a char was chosen instead of a coal to prevent problems that may arise from the evolution of tars within the gasifier bed. The char used was collected from the cyclone of a coal combustor unit. Table 1 lists both the proximate and ultimate analysis for the coal char investigated. A petrographic study showed that the char contained mainly anisotropic carbon.[5] The char was grinded and the particle fraction between 60-100mesh (150~250μm) was collected and used for the gasification experiments.

**Table 1. Proximate and ultimate analysis for the coal char investigated (dry ash basis).**

| C | H | N | S+O* | Moist. | Ash | VM | FC |
|---|---|---|---|---|---|---|---|
| 84.76 | 0.02 | 1.22 | 0.26 | 0.17 | 13.74 | 1.97 | 84.30 |

* Calculated by difference.

**Serpentine Samples**. The serpentine samples come from the Cedar Hills, USA. The particle size of the serpentine was less than 100mesh. Both the raw serpentine and activated serpentine (A-SP) samples were characterized by $N_2$ adsorption isotherms using a Quantachrome Aotusorb-1 at 77K. The raw and activated serpentine samples were placed in the fluidized bed gasifier and used simultaneously as fluidizing and carbonation agents.

**Gas analysis**. An Agilent 3000A Micro GC was used to analyze on-line the gas composition. The instrument has two channels with thermal conductivity detectors (TCD) that are capable of performing gas analyses within seconds. There is a 10m×0.32mm MolSieve 5A PLOT column and an 8m×0.32mm PLOT U column in channel A and B, respectively. Channel A uses Argon as carrier gas and Channel B uses Helium as carrier gas. The column temperature is 100 and 90°C for channel A and B, respectively.

**Gasification experiments.** The gasification tests were conducted in a lab scale bench fluidized bed gasifier. The diameter of the gasifier was 45mm. Typically, around 20g char or 20g char and 2g serpentine was put into the gasifier for each run. The reactor was heated up to the desired temperature under $N_2$, and then steam mixed with $N_2$ was fed into the gasifier to conduct the gasification reaction. In present study, the operation temperature was 950°C and the total gas flow rate was 1,475mL/min (67.73%vol steam). The composition of the produced gas was on-line analyzed using the Agilent 3000A Micro GC.

## Results and Discussion

**Characterization of raw and activated serpentine samples**. Figure 1 shows the $N_2$-77K adsorption isotherms for the raw and activated serpentine samples. For the activated serpentine, the adsorbed volume increases rapidly at low relative pressure, but it keeps increasing progressively, and there is a distinct hysteresis loop in the isotherm, which indicates that the sample porosity is a mixture of micropores (<2nm in width) and mesopores (2-50nm in width). Compared to the raw serpentine, the activated sample has developed significant microposity. The adsorbed volume increases significantly for the activated sample compared to that of the raw serpentine sample, indicating that the activation process has increased the surface area of the activated sample. Indeed, the BET surface area has gone up an order of magnitude to 142$m^2$/g compared to only~16$m^2$/g for the raw serpentine.

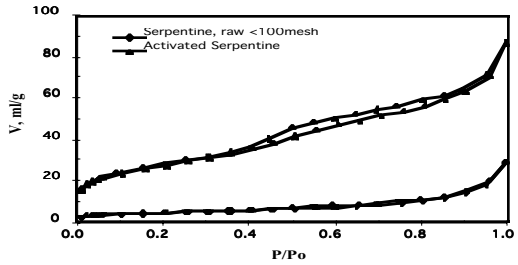


**Figure 1.** $N_2$ 77K isotherms of the raw and activated serpentine samples.

**Char gasification with and without activated serpentine addition**. Figure 2 shows the variation of the gas composition with reaction time for the char gasification experiment without serpentine. It can be seen that the concentrations of $H_2$, CO and $CO_2$ are lower than previously reported by the authors for coal gasification.[6] This could be due to the low reactivity of the coal char used. The water decomposition ratio here was just 16.67%, which is much lower than average 30% level. [6] In addition, a gasification experiment of the char mixed with activated serpentine was conducted at the same operation conditions as for the char alone gasification (Figures 3-4).

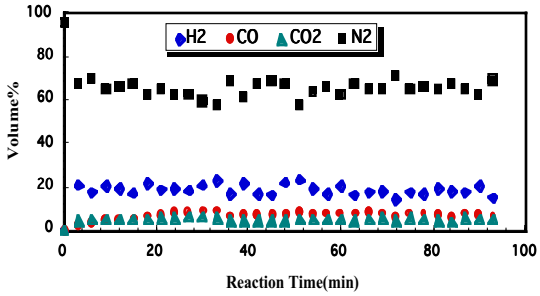


**Figure 2.** Variation of the gas concentration with reaction time for the char alone gasification experiment.

Figures 3 and 4 show the variation of $CO_2$ and $CO+H_2$ concentrations in the fuel gas with reaction time for the char and activated serpentine (A-SP) gasification compared to that of the char alone gasification. As expected, the $CO_2$ concentration decreased for the char+A-SP gasification experiment, and at the same time, the $CO+H_2$ concentration increased compared to that of the char alone gasification. During the relative steady gasification period (between 15~70mins), for the char+A-SP gasification, the average $CO_2$ concentration was 4.61%vol, and the average $CO+H_2$ concentration was 27.03%vol. For the char only gasification, the average $CO_2$ and $CO+H_2$ concentrations were 5.14%vol and 26.44%vol, respectively. Therefore, the $CO_2$ concentration decreased about 10% (from 5.14% to 4.61%), while the $CO+H_2$ concentration increased about 3.25% (from 26.44% to 27.30%) for the char gasification when activated serpentine was added. This indicates that the activated serpentine could have reduced the $CO_2$ concentration in the fuel gas, possibly due to mineral carbonation reactions. Further characterization studies of the activated serpentine minerals after gasification are being conducted to understand its role during the gasification process.

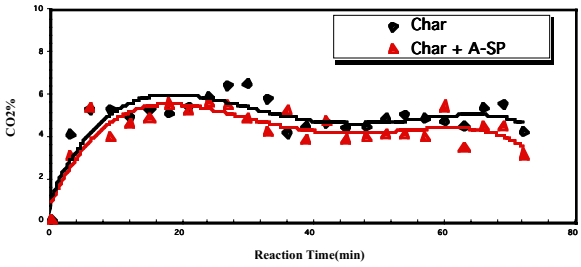


**Figure 3.** Variation of $CO_2$ concentration in the fuel gas with reaction time for the char and activated serpentine (A-SP) gasification compared to that of the char alone gasification.

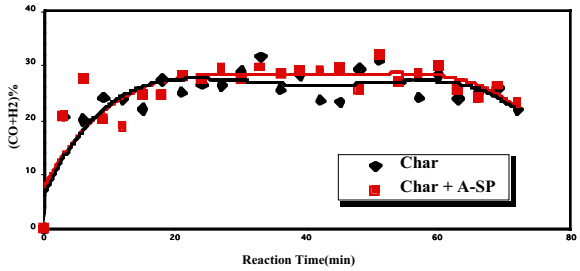


**Figure 4.** Variation of $CO+H_2$ concentrations in the fuel gas with reaction time for the char and activated serpentine (A-SP) gasification compared to that of the char alone gasification.

The water shift reaction ($H_2O + CO \leftrightarrow CO_2 + H_2$), which will determine the gas composition is a crucial reaction during gasification process. Accordingly, the rate constants of water gas shift for the char alone and char+A-SP gasification experiments were calculated, and Figure 5 shows the variation of the rate constant with reaction time. It was found that the rate constant was higher at the beginning of the gasification and then decreased slowly with gasification process, keeping virtually constant for reaction times over 75 minutes. The rate constant for the char+A-SP gasification is lower than that for the char alone gasification. The rate constants reported here are lower than the theoretical equilibrium constant (about 0.45 at 950°C). The variation of the reaction rate constant with different operation conditions indicates the magnitude of the driving force for the water gas shift reaction to occur in the positive direction. When activated serpentine is used in the gasifier bed, there is a reduction of the $CO_2$ concentration in the flue gas, suggesting that mineral carbonation of the activated serpentine during the gasification process could potentially produce high quality syngas ($CO+H_2$) with low $CO_2$ content.

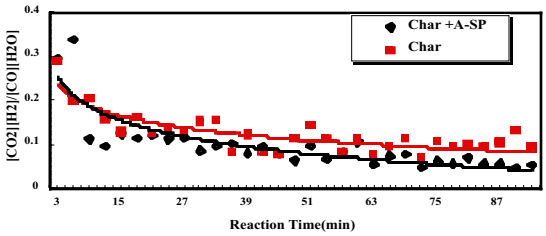


**Figure 5.** Variation of rate constant for the water shift reaction with reaction time.

## Conclusions

In this work, a lab-scale fluidized bed gasification unit was used to investigate the effect of in-bed carbon dioxide removal during coal gasification using activated serpentine. There was an improvement in the quality of the fuel gas produced (reduction of $CO_2$ concentration and an increase in the $CO+H_2$ content) when activated serpentine was added in the gasifier bed. It seems that the carbonation reaction may have occurred during the gasification process in order to reduce the $CO_2$ concentrations. Further work is underway to study the reaction mechanisms of simultaneous gasification and carbonation, and to develop a process that can integrate gasification and sequestration in order to produce high purity $H_2$ with zero emission of $CO_2$.

**Acknowledgements.** The authors wish to thank the Department of Energy and Geo-Environmental Engineering and the at Penn State University for supporting this work.

### References

1. DOE/NETL, Version 21 Program Plan, Office of Fossil Energy, U.S. DOE, 1999.
2. DOE/OS-FE, Carbon Sequestration. State of Science, Office of Fossil Energy, DOE, 1999
3. Tang, Z. and Wang, Y., *Fuel Processing Technology*, **2000**, *62(2-3)*, 137-141.
4. Maroto-Valer, M.M., Fauth, D., Kuchta, M., Zhang, Y., Andrésen, J. and Soong, Y., Eighteenth Annual International Pittsburgh Coal Conference, December 2001, Australia.
5. Maroto-Valer, M.M., Zhang, Y., Andrésen, J. and Morrison, J., Proc. of Carbon'01, July 14-19, 2001, CD paper 34-3.pdf.
6. Tang, Z., PhD dissertation, The Institute of Coal Chemistry, Chinese Academy of Sciences, 1997.

# SIMULTANEOUS CO-CARBONIZATION OF COAL AND DECANT OIL: THE EFFECT OF VARYING PROCESS PARAMETERS

*Mark Badger, Gareth Mitchell, Nate Herman, Brian Senger and Harold Schobert.*

*The Energy Institute,*
*The Pennsylvania State University,*
*University Park, PA, 16802.*

## Introduction

The practice and rationale behind the simultaneous co-carbonization of coal and decant oil, or co-coking, has been described at length elsewhere (1-5). However, the main goals of the research into co-coking at Penn State are to develop a coal-based liquid that may be upgraded into a thermally stable jet fuel, and to produce a value-added carbon product of unique properties. To this end, recent efforts have been undertaken to scale up the co-coking process from static small laboratory-scale tubing bomb experiments to a semi-continuous small pilot-scale delayed coker unit.

The delayed coker unit was designed and built in-house by researchers and staff at The Energy Institute after a similar unit operated by PARC Technical Services, Harmaville, PA. The unit has a coke drum with internal dimensions of 7.5cm ID by 102.5 cm high, giving a volume of around 4.5 liters. The unit is capable of operating under typical delayed coking process conditions. The system pressure, temperature and flow rates are monitored by a number of computer-controlled devices, and data from these devices is recorded throughout the run.

The data presented in this preprint concentrates on varying the processing parameters, and studying what affect this has on the yield and composition of the products.

## Experimental

This study used Powellton coal, that had been deep cleaned to remove the majority of mineral matter, and low sulfur decant oil. Proximate and ultimate analyses for these feedstocks are shown in Table 1.

**Table 1. Proximate and Ultimate Analysis of the Feeds Used in this Study.**

| | Coal | Decant Oil |
|---|---|---|
| Proximate analysis [a] | | |
| Ash (%) | 1.9 | 0.0 |
| Volatile matter (%) | 29.4 | - |
| Fixed carbon (%) | 68.7 | - |
| Ultimate analysis [a] | | |
| Carbon (%) | 86.3 | 89.7 |
| Hydrogen (%) | 5.2 | 9.3 |
| Nitrogen (%) | 1.5 | 0.2 |
| Sulfur (%) | 0.9 | 0.8 |
| Oxygen (by diff.) (%) | 6.1 | - |

[a]. Values reported on a dry basis

Table 2 shows experimental conditions for each of the tests performed in this study. At least two runs were performed under each of the test conditions. During each run liquid samples were taken at selected intervals. Simulated distillation (SimDis) GC was performed on these samples to study what effect the conditions had over the time of the run on the boiling range. The instrument used was a HP 5890 GC-FID fitted with a MXT-500 Sim Dist column supplied by Restek Corp. After the conclusion of the run a coring bit was used to take a representative sample of the coke bed along its entire height. Proximate and ultimate analysis was performed on the coke samples. In addition, petrographic analysis was conducted on the coke formed in the runs, following a method described previously (5).

**Table 2. Matrix of Tests Performed in this Study.**

| Coal (Wt%) | Decant Oil (Wt%) | Coke drum pressure (psig) | Water feed rate* | Sample set |
|---|---|---|---|---|
| 10 | 90 | 25 | 2% | A |
| 10 | 90 | 50 | 2% | B |
| 20 | 80 | 25 | 2% | C |
| 10 | 90 | 25 | 1% | D |

* The water feed rate is a percentage of the feedstock feed rate. For the purposes of this study the feedstock feed rate was set to 1 kg/hr. The water is used for steam injection.

## Results and Discussion

Table 3 shows data on the product yields derived for the co-coking under varying process conditions.

**Table 3. Average Product Yields for Co-coking Runs with Varying Operating Conditions.**

| Sample set | Coke yield (wt%) | Liquid yield (wt%) |
|---|---|---|
| A | 18.5 | 61.6 |
| B | 25.7 | 66.9 |
| C | 24.0 | 65.2 |
| D | 20.2 | 65.4 |

Taking sample set A as the base line set of runs observations can be made, with respect to the product yields. With an increase in coke drum pressure, there was an increase in coke yield. This is wholly consistent with results previously reported in the literature (2,6). The corresponding increase in liquid yield is an indication that there was an enhancement of cracking reactions of the higher molecular weight species. This is also exemplified in the data shown on Table 4. With an increase in coal in the feedstock, there was an increase in coke yield. This result is as expected. The ability to accurately determine how much of the coke is coal-derived has not yet been determined. The goal is to derive this value through yield calculations, with back up, concurring results from optical microscopy and other instrumental methods. With the increase in coal to the feedstock, there was an increase in the liquid yield. This result would indicate that the volatiles, from coal, evolved during the coking process were resistant to thermal cracking, and so did not decompose to gaseous compounds. A 50% decrease in water feed rate, and thus steam to the coker, resulted in an increase in coke and an increase in liquid yield. The coke increased because the lower steam rate resulted in less medium volatile compounds being swept from the coke drum. And so these medium volatiles subsequently coked. As there was an increase in liquid yield too, then the coking of the medium volatiles must have partially decomposed to intermediate lower boiling liquids, and to a lesser extent produce gaseous products.

Table 4 shows the results of SimDis GC analyses of liquid samples taken in successive periods during the different co-coking experiments.

**Table 4. Yield of Liquids in Specific Boiling Ranges Sampled at Different Times During the Co-Coking Runs.**

| | Liquid Sample | | | | | | | | |
|---|---|---|---|---|---|---|---|---|---|
| | 1 | | | 2 | | | 3 | | |
| Sample | Boiling Range (°C) | | | Boiling Range (°C) | | | Boiling Range (°C) | | |
| Set | -360 | 360-500 | 500+ | -360 | 360-500 | 500+ | -360 | 360-500 | 500+ |
| A | 22.1 | 65.8 | 8.6 | 29.5 | 61.1 | 5.8 | 31.9 | 59.3 | 5.5 |
| B | 36.9 | 51.6 | 3.9 | 38.9 | 49.0 | 4.3 | 40.3 | 50.8 | 4.7 |
| C | 31.7 | 58.7 | 4.9 | 30.2 | 58.3 | 6.2 | 28.9 | 61.7 | 7.4 |
| D | 27.3 | 63.1 | 6.6 | 28.4 | 61.6 | 5.2 | 32.4 | 58.9 | 5.7 |

For the decant oil feed –360 °C, 360-500 °C, and +500 °C cuts were 14.3%, 65.9% and 18.8%, respectively.

The most important observation that can be made from this data is that as the length of the run progresses the conversion of liquids to lighter boiling material is increased. The main reason for this phenomenon is that the coke bed facilitates the cracking of the high molecular weight species to lower molecular weight species, that boil at lower temperatures. As a run progresses the size of the bed increases, and therefore the time in which the liquids may be in contact with the bed also increases. Thus increasing the propensity for cracking reactions. The exception to this was when the coal loading was increased to 20 wt%. Although the overall liquid yield was increased, (see Table 3) the conversion to lower boiling species decreased over time. This may be because the increase in coal-derived material to liquid products may be resistant to decomposition through thermal cracking. As the majority of the coal-derived species may be of a high molecular weight this would explain the small increase in compounds boiling above 360 $^0$C as the run progressed.

Petrographic analyses of coke textures derived from coal/ decant oil blends in the laboratory-scale delayed coker, suggested that coal materials were being concentrated near the inlet of the coker and decreased in concentration with increasing bed height (see Table 5). The presence of coal in increasing concentration locally decreased the size of the isochromatic textures derived from the decant oil. The Powellton coal appeared to interact both physically and chemically with decant oil during co-coking and resulted in a significant improvement in the size of the coal-derived isochromatic textures. Changes in other operating conditions with respect to steam injection rate, drum pressure and coal addition, appeared to have an influence. Reduction of steam rate from 2.8 to 0.3 mL/min had a profound influence on increasing the size of isochromatic areas derived from the decant oil. Coke generated at the lowest steam injection rate (0.14 mL/min) and with doubled drum pressure, resulted in a significant amount of isotropic carbon derived from the decant oil. However based on earlier results, it is unclear whether operating conditions alone can be blamed for these changes in coke properties. Increasing the amount of coal in the feed to 20 wt.% had a predictable effect on coke properties, in that more enhanced coal-derived material was observed near the bottom of the core and decreased in concentration and enhancement with increasing distance from the inlet.

**Table 5. The Proportions of Textures Derived from Coal and Decant Oil Compared with the Normalized Concentration of Decant Oil Textures (Vol. %).**

| Distance from Bottom of Core, mm | % Coal derived | % Petrol. derived | % Isotropic | % Mosaic | % Small Dom.* | % Dom.* | % Flow Dom.* |
|---|---|---|---|---|---|---|---|
| **10% Powellton Coal; 20 wt% water feed rate** | | | | | | | |
| 0 -21 | 11.6 | 88.4 | 0.0 | 37.3 | 60.6 | 1.6 | 0.5 |
| 26 - 44 | 11.3 | 88.7 | 0.3 | 27.6 | 67.7 | 2.4 | 2.0 |
| **Sample Set A** | | | | | | | |
| 0 - 14.5 | 25.9 | 74.1 | 0.0 | 38.5 | 50.5 | 8.6 | 2.4 |
| 102 - 127 | 12.6 | 87.4 | 0.3 | 10.1 | 61.9 | 22.1 | 5.6 |
| 280 - 305 | 5.6 | 94.4 | 0.0 | 5.6 | 72.1 | 19.2 | 3.1 |
| 356 - 381 | 4.2 | 95.8 | 0.0 | 14.2 | 52.0 | 14.6 | 19.2 |
| **Sample Set B** | | | | | | | |
| 0 - 34 | 5.4 | 94.6 | 28.9 | 21.0 | 42.2 | 7.1 | 0.8 |
| 45 - 70 | 4.1 | 95.9 | 12.9 | 17.7 | 55.8 | 8.8 | 4.8 |
| 115 - 140 | 5.4 | 94.6 | 17.3 | 17.3 | 59.8 | 3.7 | 1.9 |
| **Sample Set C** | | | | | | | |
| 0 - 20 | 17.7 | 82.3 | 0.1 | 67.2 | 27.5 | 3.9 | 1.3 |
| 70 - 95 | 3.5 | 96.5 | 0.3 | 19.0 | 65.4 | 9.3 | 6.0 |
| 356 - 381 | 0.1 | 99.9 | 0.0 | 7.9 | 80.3 | 7.1 | 4.7 |
| **Sample Set D** | | | | | | | |
| 0 - 26 | 14.4 | 85.6 | 3.9 | 45.2 | 47.9 | 2.2 | 0.8 |
| 52 - 72 | 7.2 | 92.8 | 85.1 | 12.7 | 2.0 | 0.2 | 0.0 |
| 127 - 150 | 5.8 | 94.2 | 4.8 | 20.9 | 57.6 | 13.6 | 3.1 |

*. Dom. = Domain

## Conclusions.

Changing the experimental parameters can have a marked effect on the quality and yield of the products produced in the co-coking of coal and decant oil. Increasing the quantity of coal in the feed mix does not seem to have a detrimental effect. However, lowering the water feed rate results in a coke product of poor quality if it was to be used as a value-added carbon. Increasing the drum pressure has a disproportionate effect: The yield of liquids increases with increasing pressure, along with the yield of low boiling liquids. Conversely, the high degree of isotropic carbon reduces the quality of the coke.

## References


(1) Badger, M.W.; Fickinger, A.E.; Martin, S.C.; Mitchell, G.D.; Schobert, H.H. Prepr. Pap. - *AIE 8th Australian Coal Science Conference*, **1998,** 245.

(2) Fickinger, A.E.; Badger, M.W.; Mitchell, G.D.; Schobert, H.H. Prepr. Pap. - *ACS Div. Of Fuel Chem.* **2000**, *45*, (3), 299.

(3) Fickinger A.E. "Laboratory-Scale Coking of Coal/Petroleum Mixtures" Masters Thesis. The Pennsylvania State University. July **2000**

(4) Badger, M.W.; Fickinger, A.E.; Mitchell, G.D.; Adams, A.A.; Schobert. H.H. *Proceeding of the 26th International Technical Conference on Coal Utilization and Fuel Systems.* **2001**, 149.

(5) Badger, M.W.; Mitchell, G.D,; Karacen, C.O.; Wincek, R.T. Prepr. Pap. - *ACS Div. Of Fuel Chem.* **2001**, *46*, (2), 564.

(6) Hossain, T., Zaman, N., Jahan, S.T., Podder, J., Rashid, M.A. *J. Mech. Eng. Res. & Dev.* **1994**, *16*, 47.

# THE USE OF COAL PYROLYSIS PRODUCTS FOR THE DEVELOPMENT OF THERMALLY STABLE JET FUELS

*James J. Strohm, Suchada Butnark, Terry L. Keyser, John M. Andrésen, Mark W. Badger, Harold H. Schobert and Chunshan Song*

The Energy Institute and The Department of Energy and Geo-Environmental Engineering, The Pennsylvania State University, 209 Academic Project Bldg., University Park, PA 16802.

## Introduction

Conventional paraffin based jet fuels are solely derived from petroleum and are, in addition to serving as the fuel source, designed to act as coolants for the engines and electrical parts of the aircraft at temperatures up to 300°C (1). Lately there has been a driving force towards the development of jet planes that can operate at speeds reaching several Mach (2). The increased heat-load generated by friction with air on the body of the jet plane, the need for compressed air during combustion and higher rate of fuel injection into the engine will result in the fuel experiencing extreme temperatures when acting as coolants (3). These temperatures can reach levels around 500°C or above, and can result in severe coking of the fuel in the fuel-line although the contact time will be on the order of a few seconds. This problem has been identified especially for paraffinic based jet fuels, while naphthenic based jet fuels with a natural content of hydrogen donor compounds have shown improved thermally stability at these high temperatures (4). Correspondingly, feedstocks that can yield both naphthenes and hydrogen donor compounds will yield jet fuels with improved thermal stability.

One such route is outlined in Scheme 1. Pyrolysis of coal generates tars and liquids with a high content of aromatic compounds. From the pyrolysis product a stream with a tailored composition of aromatic compounds can be obtained. Hydrotreating and hydrogenation of such streams can yield naphthenic (cycloalkane-rich) liquids that have jet fuel characteristics. One such example is refined chemical oil (RCO) that is obtained from coal tar from by-product coke ovens (5, 6). Although aromatic streams can also be obtained from petroleum, such as light cycle oils, the high degree of alkylation of the aromatic rings lowers the thermal stability of the hydro-treated products from these streams compared to coal derived streams (7). From Scheme 1 other possible routes for the use of coal pyrolysis products are also outlined. Partial hydro-treatment of the aromatic streams from coal pyrolysis generate streams high in hydrogen donor compounds, such as tetralin, that could either be used as a fuel on its own, or used as thermal stability boosters for paraffinic derived fuels from petroleum or synthesized from coal gasification products. In addition, fully saturated naphthenic streams may also show high thermally stability in itself, or when partially mixed with the hydrogen donor containing stream.

Accordingly, in this study a refined chemical oil and two hydro-treated products with varying contents of aromatic, hydroaromatic and naphthenic compounds, were characterized and probed for their thermally stable properties. The various chemical compositions of the hydrotreated pyrolysis products were tested for their function as thermally stable jet fuels in the pyrolytic regime. In particular, the coal-derived jet fuels were able to withstand temperatures up to 820°C at short contact times even in the presence of dissolved air, while the paraffinic structure of the petroleum-derived jet fuel started decomposing below 720°C. The role of the chemical composition of the coal pyrolysis product towards the thermal stability of the resultant hydrotreated liquids was also investigated.

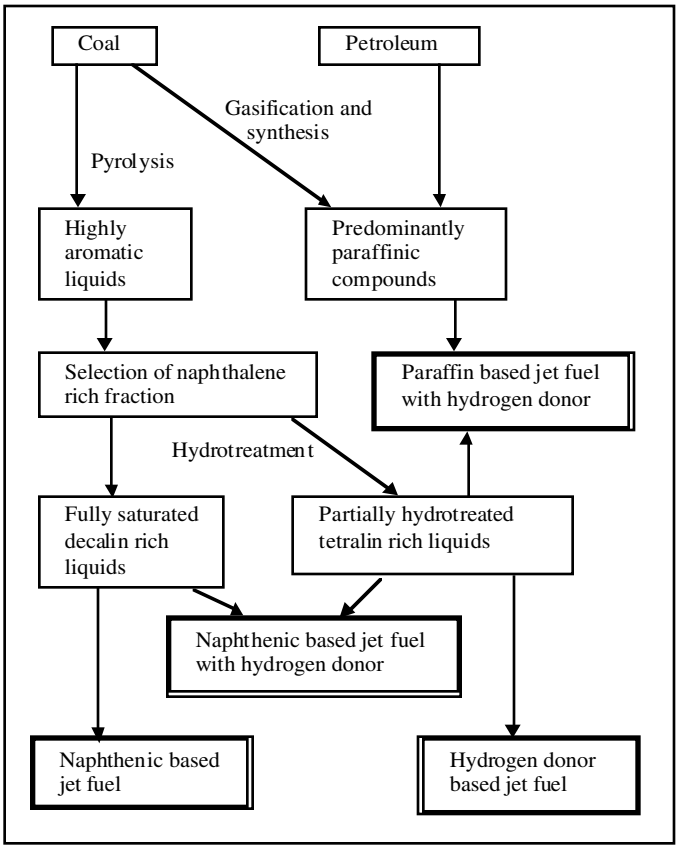


**Scheme 1.** Scheme of the possible use of coal and petroleum for the production of thermally stable jet fuels, highlighting the role of coal pyrolysis.

## Experimental

A refined chemical oil (RCO) was hydro-treated in two steps: (i) severe hydro-treatment of the RCO at 385°C to produce the partially hydro-treated HDT-RCO, and (ii) further saturation and dearomatizing at 315°C to yield SAT-RCO. The jet fuel samples were produced in a pilot plant facility by PARC (8). The flow reactor setup has been characterized elsewhere (9). The GC-MS was performed on a Shimadzu GC-174 coupled with a Shimadzu QP-5000 MS detector.

## Results and Discussion

**Characterization of samples.** The overall chemical makeup of the original refined chemical oil (RCO), its hydrotreated derivative (HDT-RCO) and its fully dearomatized fraction (SAT-RCO) is compared with the standard petroleum-derived jet fuel, JP-8P, in Figure 1. The original RCO is, as expected, highly aromatic and mainly a mixture of naphthalene and its alkylated derivatives, with about 10% alkylated benzenes and around 15% of aromatic compounds with three rings or more. The severe hydrotreatment at 385°C produces a range of hydroaromatics such as tetralin and hexahydroacenaphthalene (HDT-RCO). However, still there are some aromatic compounds remaining. Also, upon hydrotreatment virtually all of the 3+ aromatic rings compounds have one or more of the rings hydrogenated, transforming them into hydro-aromatics. A similar change was found for the naphthalenes, where the major hydroaromatic was tetralin and its alkylated derivatives. The alkyl-benzenes were transformed to cyclo-alkanes. When fully

dearomatized into SAT-RCO, essentially all the aromatics and hydroaromatics have been converted to cyclo-alkanes, which account for over 98% of this fraction. The dearomatization of the coal-derived liquid causes a dramatic conversion to decalins, mostly the *trans*-decalin isomer, but also a considerable content of the *cis*- isomer. Figure 1 also compares the chemical structure of the petroleum-derived jet fuel, JP-8P to that of the three coal-derived streams. As expected, the JP-8P is dominated by a high content of long-chain paraffins. Also, JP-8P does not contain any hydro-aromatic structures such as tetralin, and all the aromatic compounds are alkylated benzenes or alkylated naphthalenes.

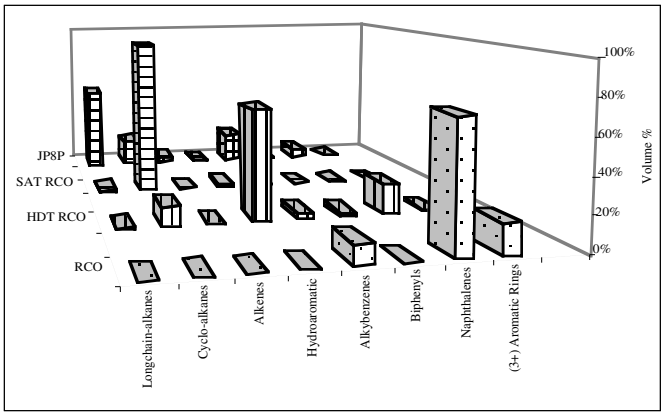


**Figure 1.** The overall chemical makeup of the coal-derived refined chemical oil (RCO), its hydro-treated (HDT-RCO) and fully dearomatized (SAT-RCO) fractions, compared to that of the standard petroleum derived jet fuel, JP-8P.

**Thermal stability of the jet fuels.** Figure 2 shows the changes in the chemical composition as detected by GC/MS of the saturated RCO stream when purged with oxygen and heated to 771°C in the flow reactor. The coal-derived fuel, SAT RCO, can be heated to these temperatures with very little thermal decomposition of the structure.

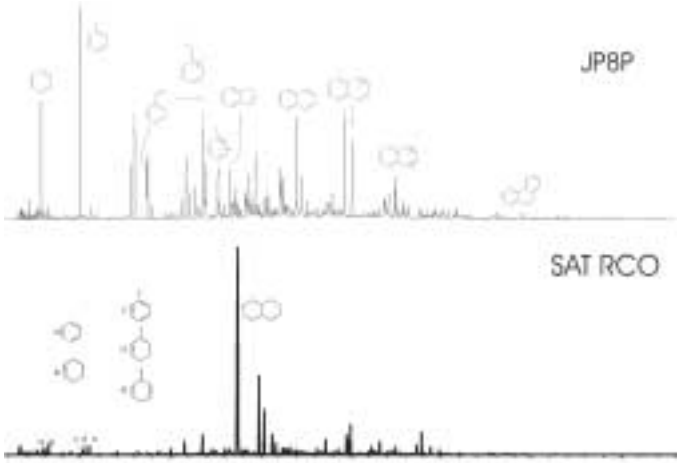


**Figure 2.** The change in chemical composition as detected by GC/MS of the saturated RCO stream when purged with oxygen and heated to 771°C in flow reactor.

In comparison, when the petroleum-derived jet fuel JP-8P is purged with oxygen and heated to 771°C in the flow reactor severe thermal cracking is observed resulting in a nearly complete transformation of long-chain paraffins into aromatic compounds.

**Solid deposition in fuel line.** Figure 3 compares the changes in coke deposits along the fuel line of the flow-reactor related to the bulk-fuel temperature. Very little solid deposition is observed in the tube in the temperature range 25 to 450°C. This was unexpected, since the fuels may form gums, especially JP-8P, due to the presence of oxygen in the fuel. The gums are formed in the autoxidative regime from 150 to 350°C. However, due to the high flow rate in the system (LHSP of 450) the gums may not precipitate before 500°C. This can explain the growth in solid deposit peak for JP-8P at 700°C and the subsequent decrease at 750°C before pyrolytic solid deposition increases rapidly at higher temperatures. The coal-derived SAT-RCO jet fuel may have formed some gums at 550°C but does not form pyrolytic solid deposit before 800°C.

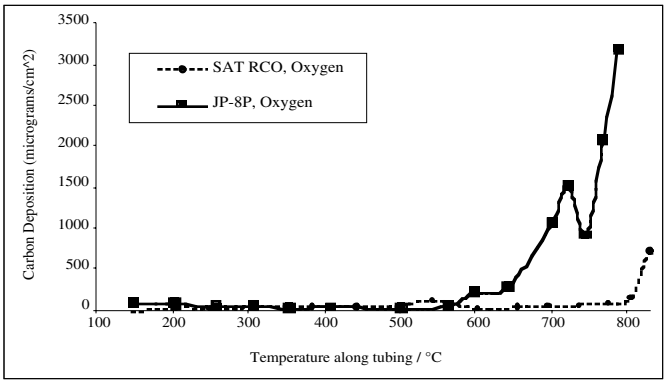


**Figure 3.** Changes in coke deposits along the fuel line of the flow-reactor related to the bulk-fuel temperature.

## Conclusions

A jet fuel derived from a refined chemical oil, obtained from coal pyrolysis, was found to be thermally stable up to 771°C in a flow-reactor. Compared to the petroleum-derived jet fuel, JP-8P, that showed extensive thermal cracking at these temperatures, the coal-derived jet fuel was superior in suppressing the formation of solid deposit in the fuel line.

**Acknowledgements.** The authors wish to thank the USAF/WPAFB for their support, Koppers and PARC for the RCO sample and preparation.

## References

(1) Yoon, E.M.; Selvaraj, L.; Song, C.; Stallman, J.B and Coleman, M.M., Energy & Fuels, **1996**,*10*, 806.
(2) Ben-Yakar, A. and Hanson, R.K., J. Propulsion and Power, **2001**, *17 (4)*, 869.
(3) Edwards, T., Prepr. Pap. - *Am. Chem. Soc., Div. Petr. Chem.*, **1996**, *41(2)*, 481.
(4) Song, C.; Eser, S.; Schobert, H.H.; and Hatcher, P.G. Energy & Fuels, **1993**, *7*, 234.
(5) Butnark, S.; Badger, M.W.; Schobert, H.H., Prepr. Pap. - *Am. Chem. Soc., Div. Fuel Chem.*, **1999**, *44* (3), 662.
(6) Butnark, S., Hydrogenation of Coal Tar Fractions and Refinery Streams. Master Thesis. Pennsylvania State University, December 1999.
(7) Andrésen; J.M., Strohm; J.J, Sun, L. and Song, C, Energy & Fuels, **2001**, *15*, 714.
(8) Wilson, G. R. Project Report on AFOSR-Subcontract for Advanced Thermally Stable Coal-Based Jet Fuels for the Pennsylvania State University. PARC Technical Services Inc. (Pittsburgh, PA) to Pennsylvania State University, May 2000.
(9) Andrésen, J.M.; Strohm, J.J.; Boyer, M. L.; Song, C.; Schobert, H.H.; and Butnark, S., *Am. Chem. Soc., Div. Fuel Chem.*, **2001**, 46(1), 208.

# VOLATILIZATION OF Na DURING PYROLYSIS OF A VICTORIAN BROWN COAL AT ELEVATED PRESSURES

*Chirag Sathe[a,b], Jun-ichiro Hayashi[b], Chun-Zhu Li[a] and Tadatoshi Chiba[b]*

[a]CRC for Clean Power from Lignite, Department of Chemical Engineering, Monash University, Clayton, Australia
[b]Center for Advanced Research of Energy Technology Hokkaido University, Sapporo, Japan

## Introduction

Volatilization of Na during pyrolysis/gasification has been known to cause severe problems of erosion/corrosion of heat-exchanger tubes and high-temperature rotating parts in a gas turbine, affecting the steady operation of the plant. On the other hand, retention of Na in the char would enhance combustion/gasification processes due to its catalytic activity. The volatilization of Na is likely to be dependent on the reaction conditions. This paper examines the effects of changes in pressure, heating rate and temperature on the release of Na during pyrolysis of a Victorian brown coal (Loy Yang).

## Experimental

**Coal sample.** A sample of "as-mined" brown coal was obtained from the Loy Yang field in Latrobe Valley, Australia. The sample was partially dried at low temperature (<35°C) and then pulverized and sieved to obtain a fraction sample of particle sizes between 106 and 150 µm. The properties of the coal sample are: C, 68.5; H, 4.8; N, 0.6 and S, 0.3 wt% on a daf basis with 0.13 wt% of Na (db).

**Pyrolysis**. Pyrolysis experiments were carried out in a wire-mesh reactor[1]. For experiments at elevated pressures, a reactor vessel made of stainless steel (instead of glass) was used together with a specially designed gas distributor and a tar trap. Less than 10 mg of the air-dried sample was used in each experiment. The details of tar collection, char and tar quantification have been given elsewhere[2,3]. All the pyrolysis experiments were carried out in helium (purity >99.999%). A gas flow rate of 2.5 L $min^{-1}$ (measured at 25°C and 1 bar) was used for experiments at atmospheric pressure. For experiments at pressures from 6 bar to 20 bar, a gas flow rate of 4 L $min^{-1}$ (measured at 25°C and 1 bar) was used to maintain an upward flow direction of the volatiles. Experiments using a higher flow rate of 8 L $min^{-1}$ at elevated pressures (20 bar) did not show any discernible changes in product yields. For very high pressure up to 61 bar, a gas flow rate of 10 L $min^{-1}$ was used.

**Quantification of Na.** Detailed procedure for the quantification of Na is given elsewhere[2]. In brief, after the pyrolysis experiment, a portion of the char was ashed in a thermogravimetric analyzer at 600°C (with 30 min holding time) in $O_2$. The ashing conditions were controlled to ensure complete combustion without ignition[2]. The ash was then digested with a mixture of $HNO_3$ and HF solution. After evaporating $HNO_3$ and HF the sample was re-dissolved in 20 mM $CH_3SO_3H$ prior to injection into an ion chromatograph to quantify Na concentrations.

## Results and Discussion

Pyrolysis experiments using the raw coal sample were carried out at pressures of 1, 3, 6, 11, 20, 36 and 61 bar. Two heating rates were used: 1 and 1000°C $s^{-1}$ with a holding time of 10 s. As indicated previously[4], the introduction of pressure greatly affects the mass-transport mechanism of volatiles and changes the tar yield. A brief summary on the effect of pressure on the tar yield is given here in the form of Figure 1 at 700 and 900°C. At the fast heating rate of 1000°C $s^{-1}$ the tar yield decreases with increases in pressure up to 11 bar. Further increase in pressure to 20 bar results in substantial increases in the tar yield. At a slow heating rate of 1°C $s^{-1}$, the tar yield remains unaffected by pressure up to 6 bar, but nearly doubles at 11 bar and remains unchanged up to 20 bar.

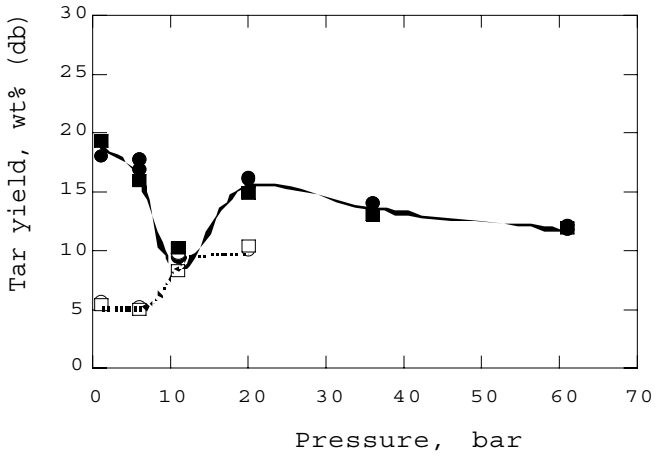


**Figure 1.** Effect of pressure on the tar yield at 700 (l and °) and 900°C (n and o) with a holding time of 10 s at: 1000°C $s^{-1}$ (filled symbol) and 1°C $s^{-1}$ (open symbol).

In our previous study[2] at atmospheric pressure, the volatilization of Na was found to be a function of temperature alone. Changes in the heating rate (1 and 1000°C $s^{-1}$) had no apparent effect on the release of Na. When the pressure is increased in the present study from 1 to 11 bar at 700°C at the fast heating rate, the Na retention in the char decreases gradually, as shown in Figure 2. When the pressure is increased to 20 bar, the Na retention increases substantially which is followed by no essential increase with pressure up to 61 bar. More than 85% of Na present in the coal sample is retained in the char at pressures of 20 bar and higher.

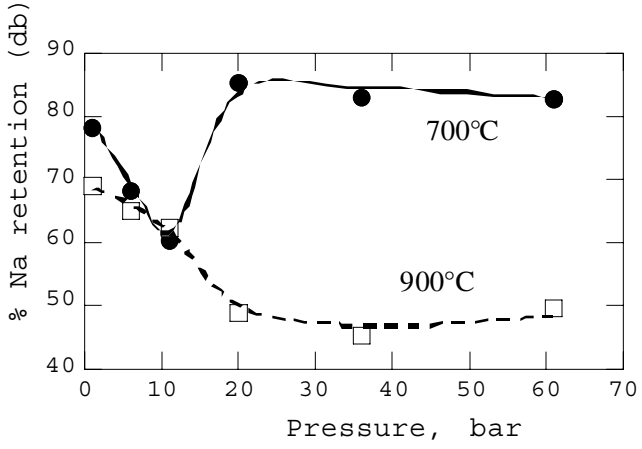


**Figure 2.** Na retention as a function of pressure at 700 and 900'C at a fast heating rate of 1000°C $s^{-1}$ with a holding time of 10 s.

Interestingly, Figs. 1 and 2 suggest that at 700°C the Na retention followed the path of the tar yield with changes in pressure. At a higher temperature of 900°C, the Na retention shows similar behavior to that at 700°C with increases in pressure up to

11 bar. However, the difference between the Na retention at 700 and 900°C decreases with increases in pressure. At 11 bar, the Na retention is same at both temperatures. Further increase in pressure to 20 bar at 900°C causes a significant reduction in the retention and remains unchanged with further increases in pressure up to 61 bar. It appears from Figs. 1 and 2 that at a higher temperature of 900°C, the temperature has played a significant role in the volatilization of Na from the coal.

When the coal particles are heated slowly at 1°C $s^{-1}$, the Na retention for both temperatures decreases with pressure to 6 bar and then remains nearly unchanged up to 11 bar, as shown in Figure 3. However, at 20 bar the retention increases and matches the value at 1 bar. This behavior of Na at 900°C is in sharp contrast to that at fast heating rate. It is also to be noted that the difference between the retention at 700 and 900°C remained nearly unchanged with increasing pressure.

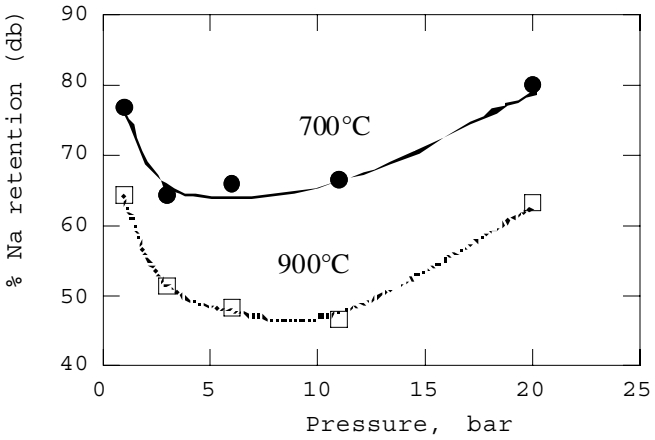


**Figure 3.** Na retention as a function of pressure at 700 and 900°C at a slow heating rate of 1°C $s^{-1}$ with a holding time of 10 s.

It is supposed that when the generation of volatiles in the particle is rapid the evolution of the volatiles out of the particle can be affected by pressure[5]. As discussed in detail elsewhere[4], with changes in pressure, the diffusion flow due to the concentration gradient and/or the forced flow due to the pressure gradient would be the main mass transport mechanism for the release of volatiles out of the particle during rapid pyrolysis. This in turn could affect the release of alkali and alkaline earth metallic species (AAEM). Thus, the release of AAEM species was speculated to depend on their transformation during pyrolysis.

It is known that the carboxylates in coal will undergo decomposition at relatively low temperatures[6]. In the absence of oxygen, some AAEM species associated with the $-COO^-$ groups might leave the particle together with the –COO group. With the release of $CO_2$, Na originally associated with a –COO group might still be bonded to coal/char matrix (CM),

$$(\text{-COO-Na}) + (\text{CM'}) \Rightarrow \text{CM-Na} + CO_2 \quad (1)$$

The strength of this newly formed bond will depend on the temperature alone. Increasing temperature would generate volatile matter (VM') from the coal/char matrix,

$$\text{CM-VM} \Rightarrow \text{CM'} + \text{VM'} \quad (2)$$

and could also break the bond between CM and Na,

$$\text{CM-Na} \Rightarrow \text{CM'} + \text{Na'} \quad (3)$$

In the diffusion controlled mass transport regime, the concentration of the VM inside the particle increases with increasing pressure. This will allow for the further interaction between the VM' and Na',

$$\text{VM'} + \text{Na'} \Rightarrow \text{VM-Na} \quad (4)$$

It is speculated that the Na could be released along with VM. The chances of Na being released by reaction (3), even after the completion of the release of tar and major volatiles, are not excluded. On the other hand, if the forced flow is the main controlling mass transport mechanism for the release of volatiles, the concentration as well as the time spend by VM' inside the particle would reduce considerably. This, in turn, would reduce the possibility of the interaction between VM' and Na'.

At 700°C the thermal dissociation (reaction 3) would not be an important process for the volatilization of Na. In the diffusion controlled mass transport process regime (up to 11 bar), reactions (2) and (4) would play a vital role and result in more release of Na with increasing pressure. When forced flow becomes the main mass transport mechanism (at 20 bar), there are neither enough Na' species and/or the VM' nor the time available for the progress of reaction (4) to cause volatilization of Na. The Na retention increased substantially when the pressure is increased to 20 bar (Fig 2). At 900°C, the reaction (3) would intensify and irrespective of the mass transport regime would cause further volatilization of Na with increasing pressure (up to 20 bar). At higher pressures (36 and 61 bar), the data in Fig. 2 suggest that the release of Na has reached a plateau value at 900°C.

When the generation of volatiles is slow and is the rate-limiting process, as in the case with 1°C $s^{-1}$, increasing pressure would further increase the concentration of VM inside the particle. The net result of reactions (2), (3) and (4) is a gradual release of Na with increasing pressure. The data in Figs. 1 and 3 for 20 bar are somewhat ambiguous. The slow generation of volatiles is thought to negate the effect of increasing pressure on the release of volatiles. However, the increase in the tar yield as well as the Na retention at 20 bar suggest the forced flow could be the main mass transport mechanism for the release of volatiles, resulting in higher retention of Na during pyrolysis. Further work is being carried out to understand the effect of pressure on the release of Na during slow heating.

## Conclusions

Tar yield is found to be sensitive to changes in pressure and heating rate. Volatilization of Na is found to depend on pressure, temperature and heating rate. At atmospheric pressure, the release of Na is only temperature dependent. Increasing pressure alters the mass transport mechanism of the generated volatiles and in turn affects the volatilization of Na. At fast heating rate, higher pressure and higher temperature result in substantial volatilization of Na. At slow heating rate, the volatilization of Na is mainly a function of temperature.

**Acknowledgement.** The financial and other support received for this research from the Cooperative Research Center (CRC) for Clean Power from Lignite (Australia) is gratefully acknowledged. The authors also thank the partial financial support by the New Energy and Industrial Technology Development Organisation (NEDO) in Japan.

## References

(1) Sathe, C.; Pang, Y.; and Li, C.-Z. *Energy & fuels*, **1999**, *13*, 748-755.
(2) Li, C.-Z.; Sathe, C.; Kershaw, J. R.; and Pang, Y. *Fuel*, **2000**, *79*, 427.
(3) Kershaw, J. R.; Sathe, C.; Hayashi, J.-i.; Li, C.-Z; and Chiba, T. *Energy & Fuels*, **2000**, *14*, 476-482.
(4) Sathe, C.; Hayashi, J.-i.; Li, C.-Z. submitted to *Fuel*, **2001**.
(5) Gavalas, G.R. Coal Pyrolysis, Elsevier Scientific Publication: Amsterdam, 1982; Chapter 5.
(6) Schafer, H.N.S. The Science of Victorian brown coal, Editor, Durie, R.A.; Butterworth-Heinmann, 1991; Chapter 7.